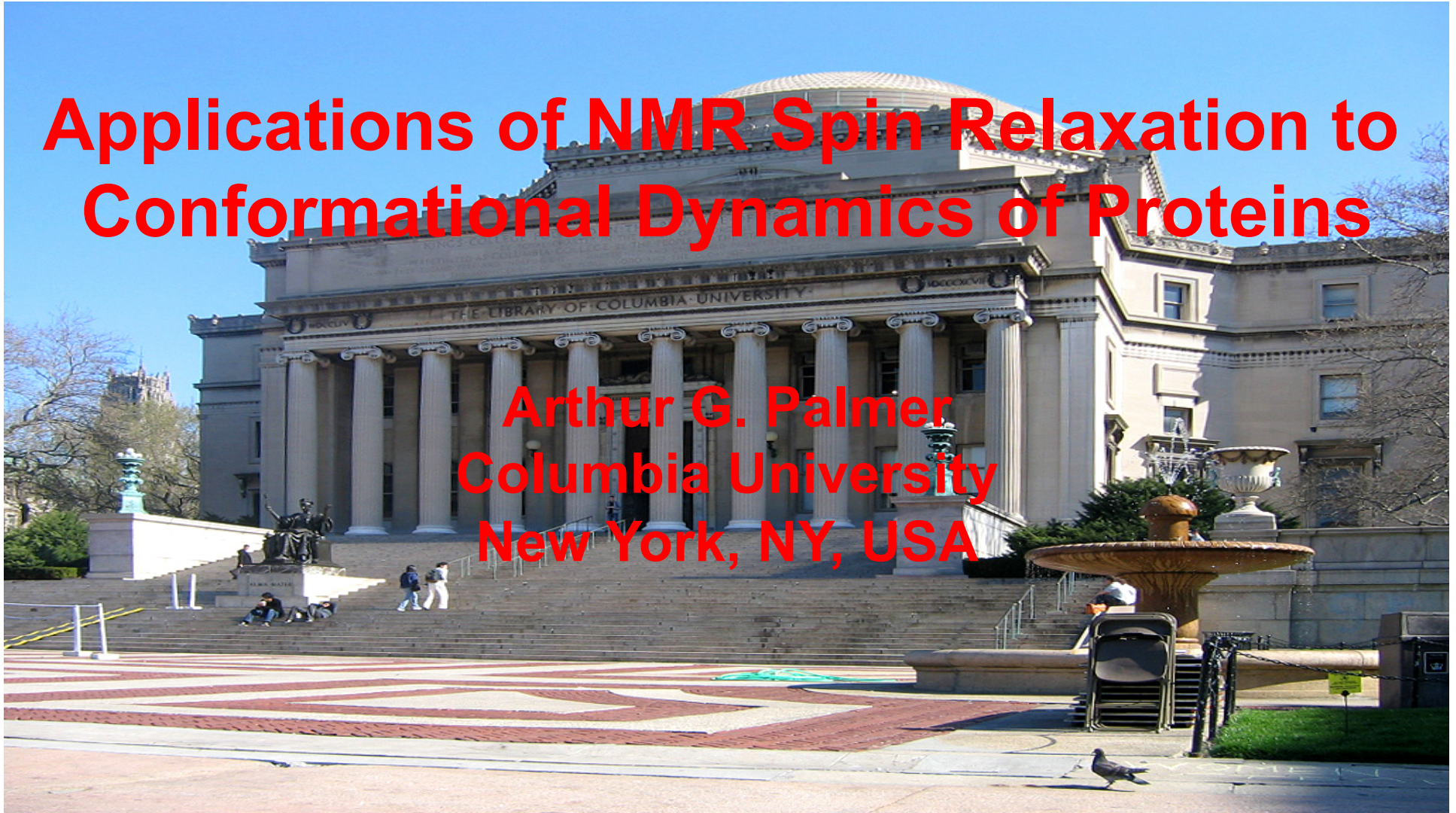


Applications of NMR Spin Relaxation to Conformational Dynamics of Proteins

Arthur G. Palmer
Columbia University
New York, NY, USA



References

NMR Spectroscopy: NMR Relaxation Methods, Comprehensive Biophysics, Vol 1, Biophysical Techniques for Structural Characterization of Macro-molecules, Oxford: Academic Press, 2012. pp. 216-244.

Enzyme dynamics from NMR spectroscopy, *Acc. Chem. Res.* 48, 457-465 (2015).

Chemical exchange in biomacromolecules: Past, present, future, *J. Magn. Reson.* 241, 3-17 (2014).

Experimental Methods

Laboratory Frame Relaxation Techniques

Generalized order parameters

Diffusion tensors

Rotating Frame Relaxation Techniques

Chemical exchange kinetics

Other approaches (not discussed)

Amide proton-solvent exchange

Averaging of scalar and dipolar couplings

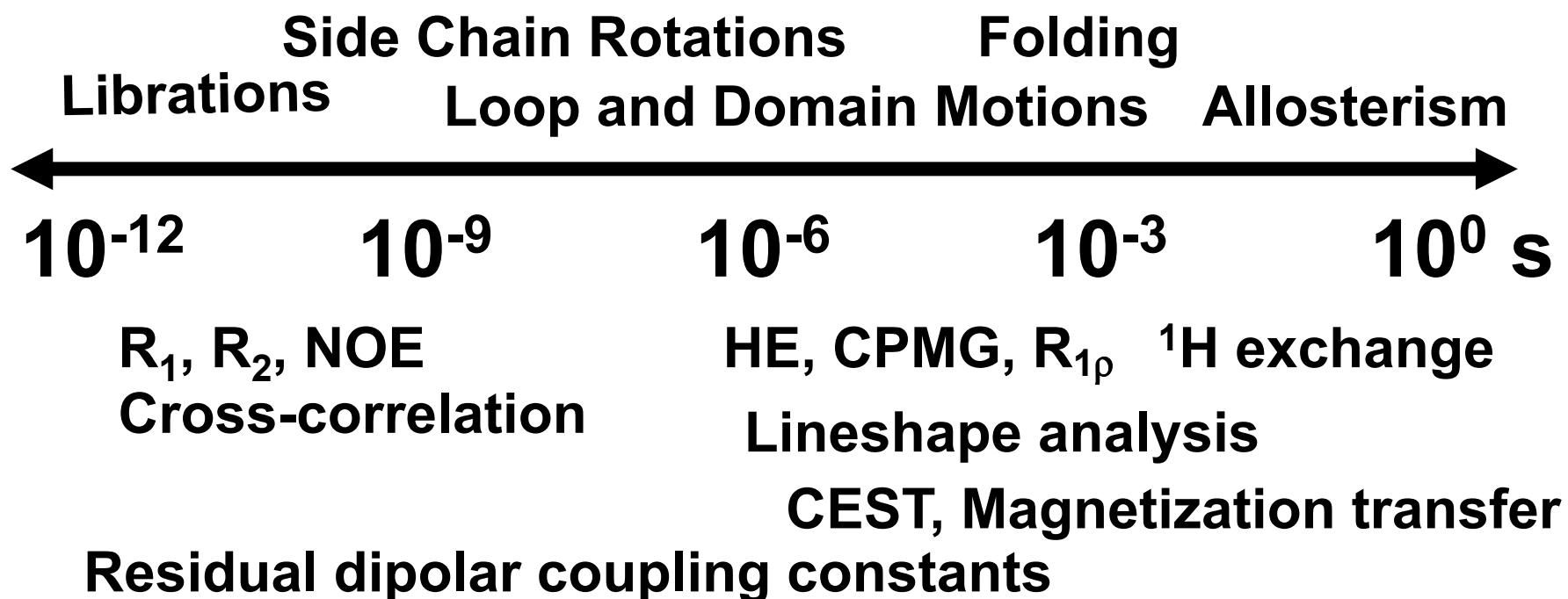
Why Study Protein Dynamics?

Information for structure determination: which regions of molecule are really disordered.

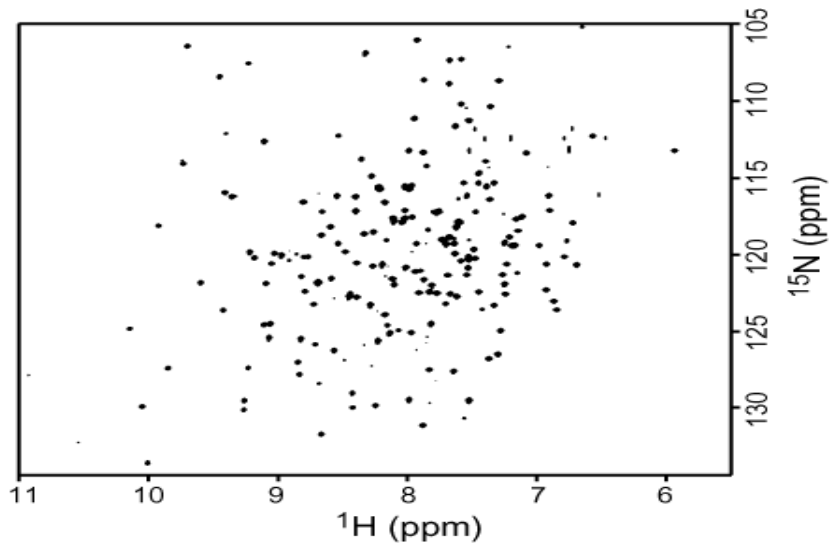
Biophysical studies of protein statistical mechanical properties: kinetics, energetics and mechanisms of equilibrium fluctuations.

Biological applications: folding, ligand-binding, allostereism and catalysis.

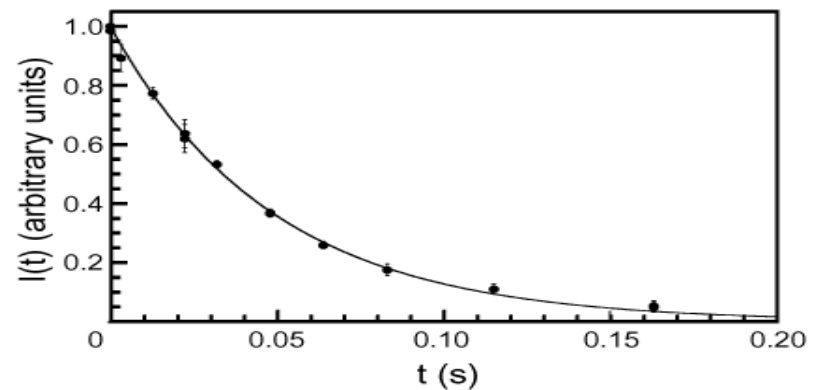
Time Scales for Protein Dynamics



Site-resolved relaxation rate constants provide site-specific probes of dynamics



| | | | | |
|-------------|-------------------|-------------------|--------|---------------|
| Preparation | Relaxation t | Labeling t_1 | Mixing | Acq. t_2 |
|-------------|-------------------|-------------------|--------|---------------|



Relaxation rate constants are determined from intensity decays in a time series of 2D NMR spectra for different values of t

Critical Initial Considerations

Experiments conducted at different magnetic field strengths are very useful for increasing information content.

Always dilute the sample and run an R_2 measurement to check for aggregation.

Control sample temperature: use compensation pulses or fields during recycle delay so total rf power deposited in sample is independent of relaxation delay [A. C. Wang, A. Bax, *J. Biomol. NMR* **3**, 715-720 (1993)].

Control spectrometer room temperature as closely as possible (monitor temperature during experiments).

Error analysis is crucial: as many duplicate measurements as you can afford and careful data analysis.

Fast Dynamics (ps-ns)

Experiments are well-developed for ^{15}N -H and $^{13}\text{CH}_2\text{D}$ methyl groups, giving access to probes of backbone and side chain motions.

Laboratory frame relaxation rate measurements (R_1 , R_2 , R_{1r} , steady state NOE, relaxation interference rate constants).

Relaxation rate constants are linear combinations of the spectral density function, $J(\omega)$, at characteristic values of ω .

Lipari-Szabo model-free formalism (and its variants), SRLS, or computational simulations are used to interpret $J(\omega)$.

Internal motions on time scales faster than overall rotational diffusion (very accurate measurements are necessary for motions comparable to or slower than overall motion).

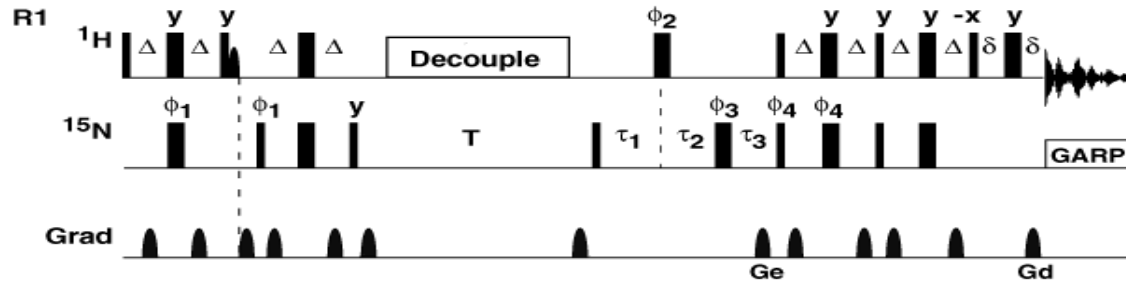
(Hopefully) Useful Points

Spectral density mapping as an intermediate step in the analysis allows more direct visualization of the fitting process compared with direct fitting of the relaxation rate constants. This is particularly useful for data acquired at >1 field.

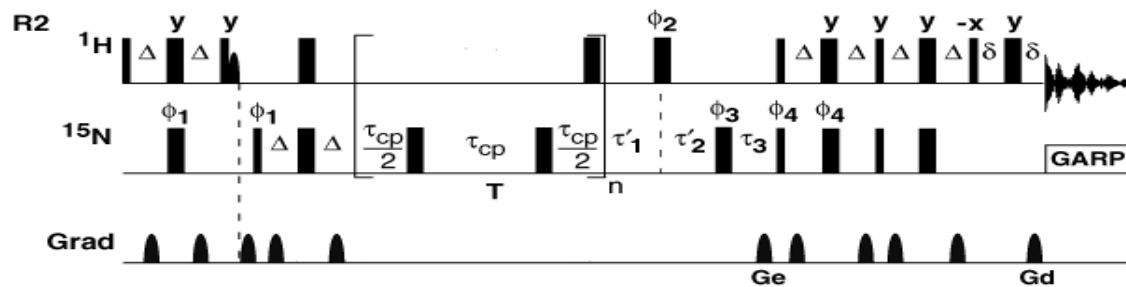
Determine R_2^0 (exchange-free transverse relaxation rate constant) from relaxation interference rate constant, η_{xy} , or B_0 dependence of $R_2 - R_1/2$ so that slow processes do not corrupt the analysis.

CPMG and $R_{1\rho}$ experiments are very similar theoretically and with appropriate experimental care (accurate schemes for decoupling), either can be used for R_2 . In both cases, correct for resonance offset effects during data analysis.

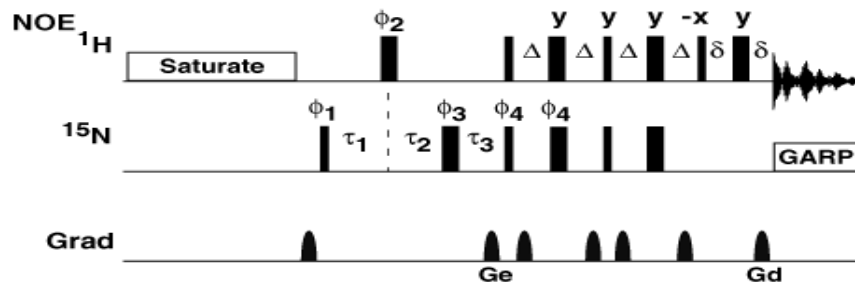
Pulse sequences for ^{15}N Relaxation



$$I(T) = I(0)\exp(-R_1T)$$



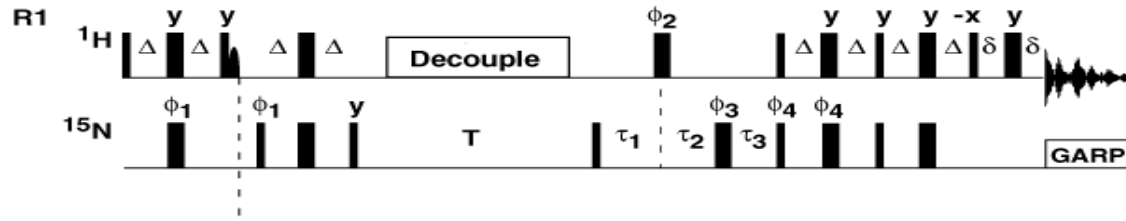
$$I(T) = I(0)\exp(-R_2T)$$



$$\text{NOE} = I_{\text{NOE}} / I_{\text{CONTROL}}$$

N. A. Farrow, et al., *Biochemistry*
33, 5984-6003 (1994).

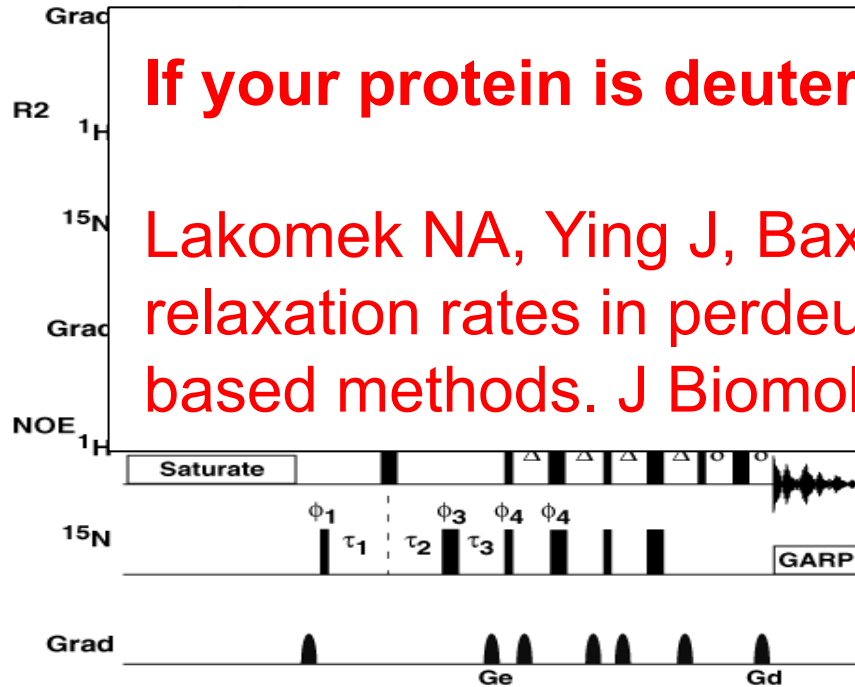
Pulse sequences for ^{15}N Relaxation



$$I(T) = I(0)\exp(-R_1T)$$

If your protein is deuterated (a good idea):

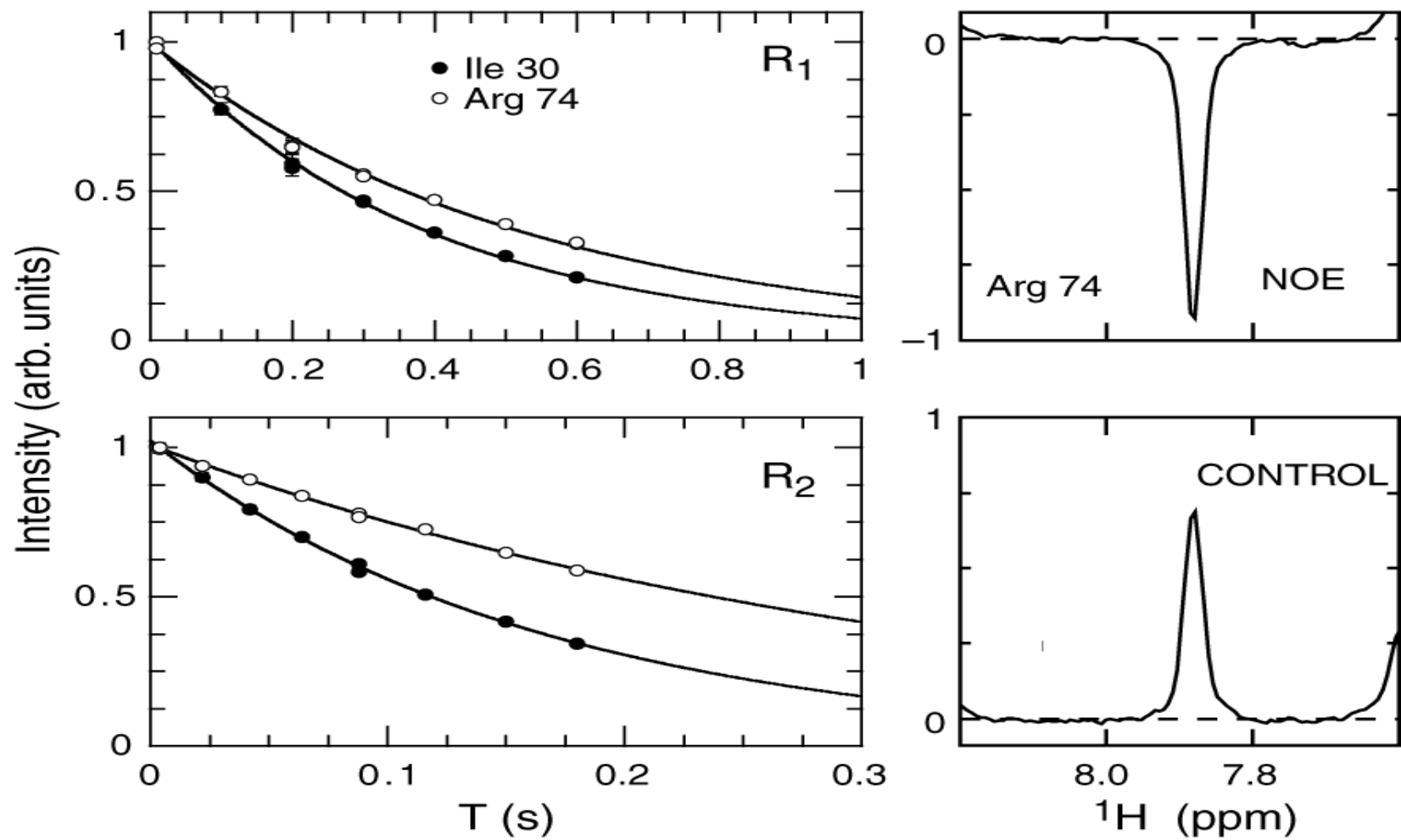
Lakomek NA, Ying J, Bax A. Measurement of ^{15}N relaxation rates in perdeuterated proteins by TROSY-based methods. *J Biomol NMR*, 2012, 53:209-21.



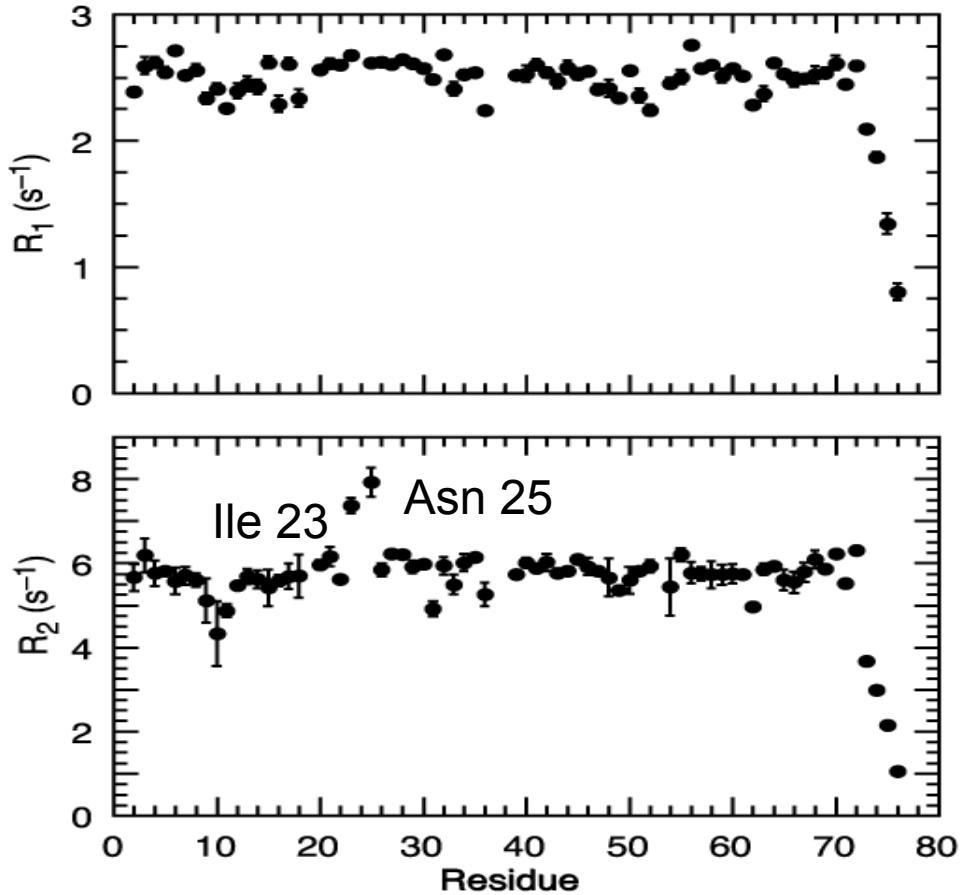
$$\text{NOE} = I_{\text{NOE}} / I_{\text{CONTROL}}$$

N. A. Farrow, et al., *Biochemistry* 33, 5984-6003 (1994).

Laboratory Frame Relaxation Data for Ubiquitin



Relaxation Rate Constants for Ubiquitin

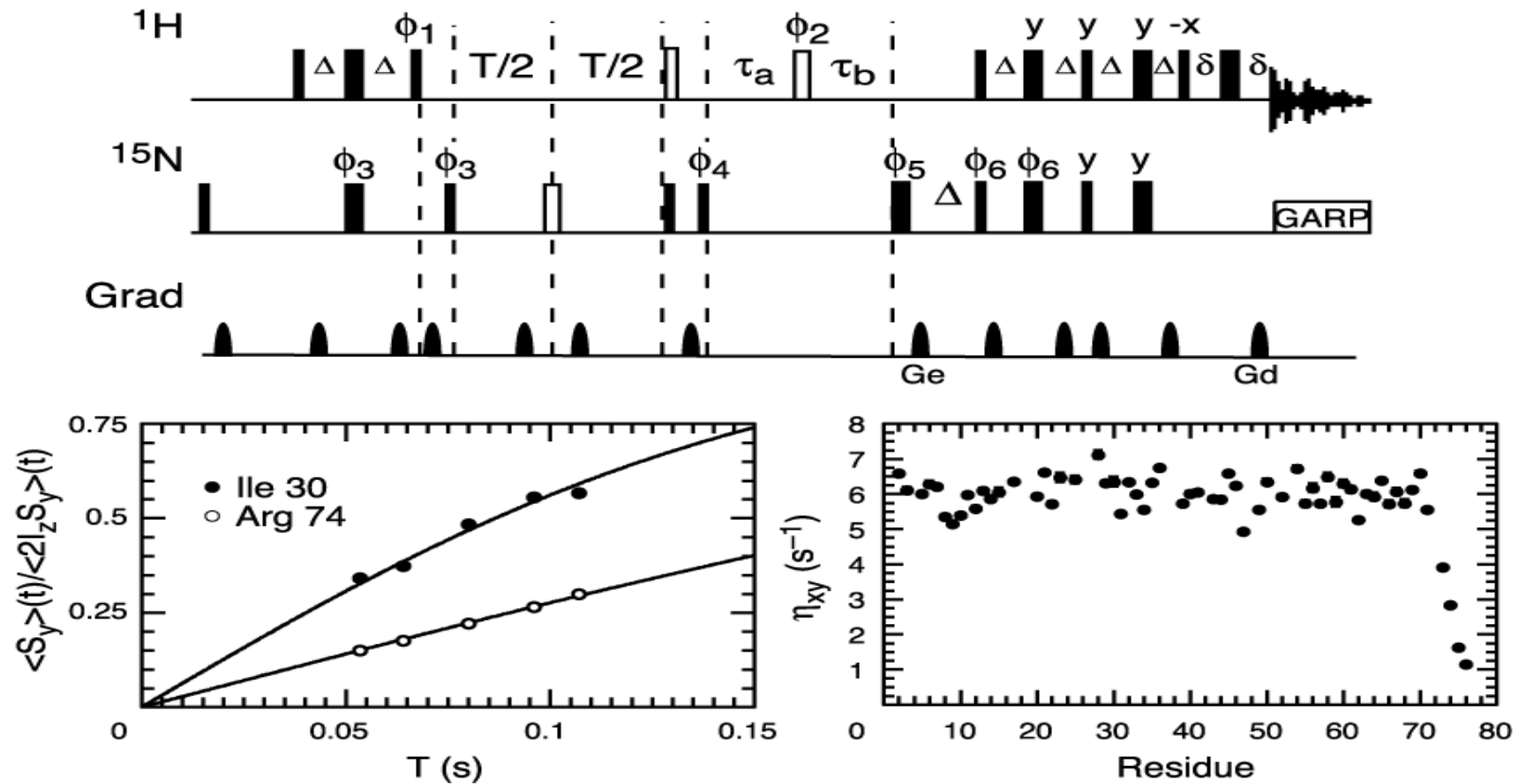


Reduced R_2 and NOE: ps-ns internal motions.

Increased R_2 : Chemical exchange broadening.

Diffusion anisotropy is a confounding factor.

Relaxation interference for Ubiquitin

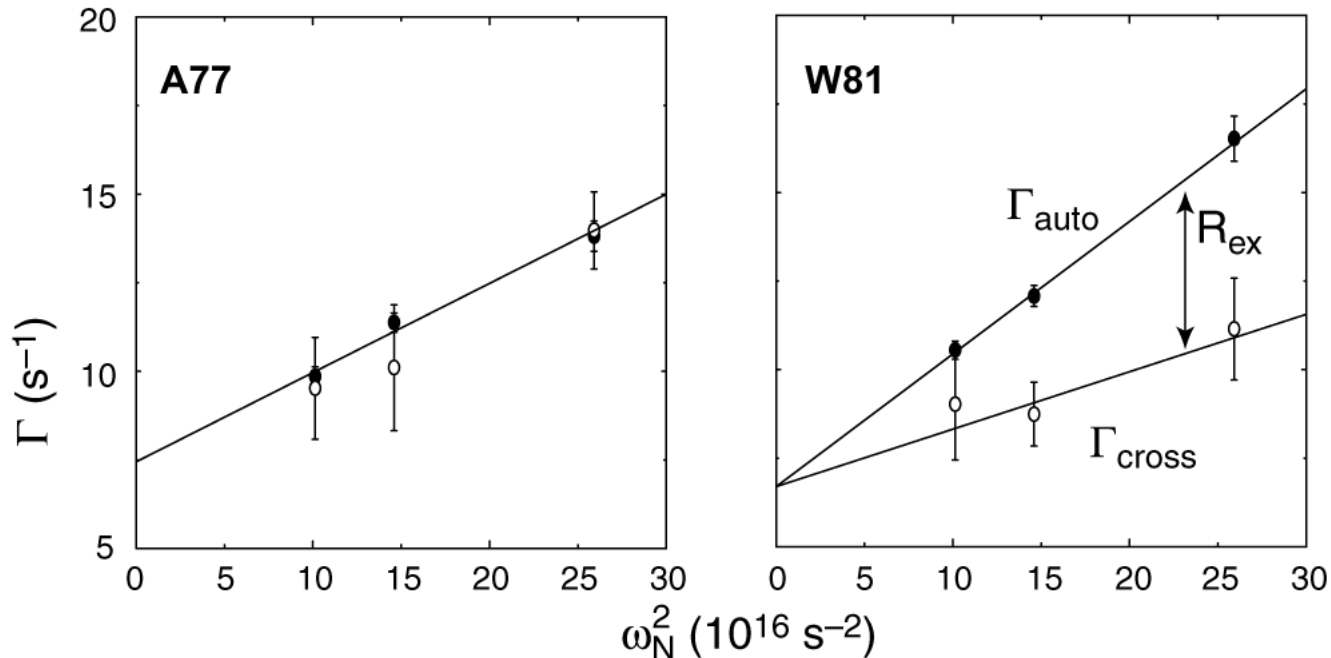


C. D. Kroenke, et al., *J. Am. Chem. Soc.* 120, 7905-7915 (1998).

Field Dependence of R_2 to Detect Chemical Exchange

$$\Gamma_{\text{auto}} = R_2 - R_1/2 = \Gamma_{\text{cross}} + (dR_{\text{ex}}/d\omega_N^2) \omega_N^2$$

$$\Gamma_{\text{cross}} = \eta_{xy} - \eta_z/2 \quad (\eta_{xy} \text{ and } \eta_z \text{ are interference rate constants})$$



C. D. Kroenke, et al., JACS (1999) 121:10119-10125

Model-free formalism for Axial Diffusion Tensor

$$J(\omega) = \frac{2}{5} \sum_{j=0}^2 A_j \left[\frac{S^2 \tau_j}{1 + \omega^2 \tau_j^2} + \frac{(1 - S^2) \tau'_j}{1 + \omega^2 \tau_j'^2} \right]$$

$$\tau_j^{-1} = 6D_{\perp} - j^2(D_{\perp} - D_{\parallel})$$

$$\tau'_j = (1/\tau_j + 1/\tau_e)^{-1}$$

$$A_0 = (3\cos^2\theta - 1)^2/4 \quad A_1 = 3\sin^2\theta\cos^2\theta \quad A_2 = (3/4)\sin^4\theta$$

D_{\parallel} and D_{\perp} are the components of an axially symmetric diffusion tensor

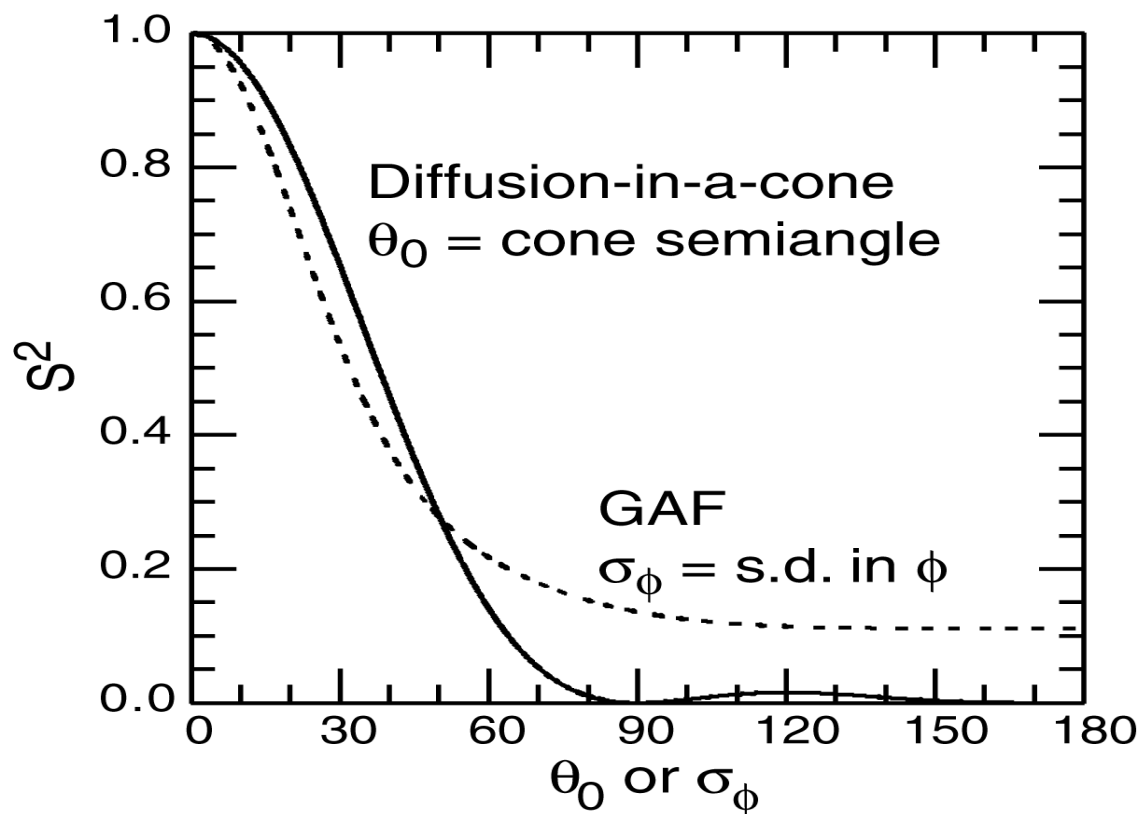
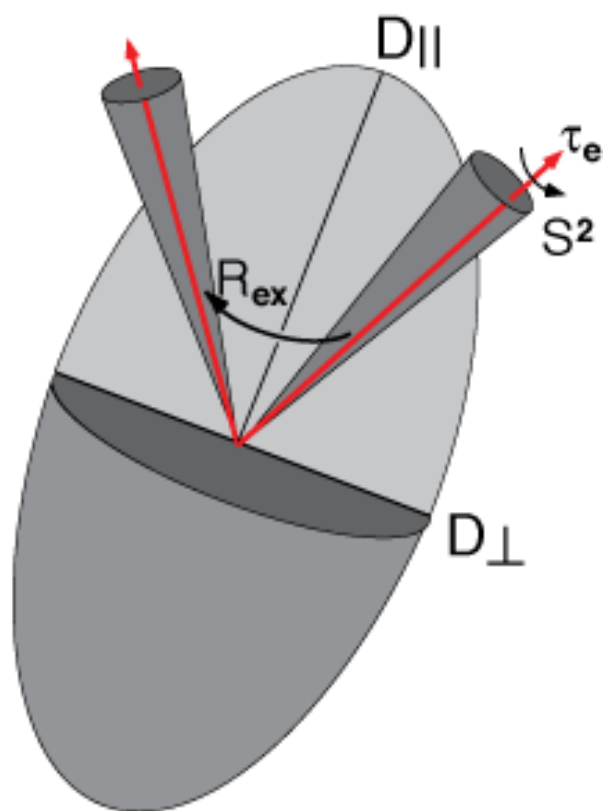
θ is the angle between the unique axis of the diffusion tensor

and the equilibrium orientation of the NH vector, $\mu(t)$

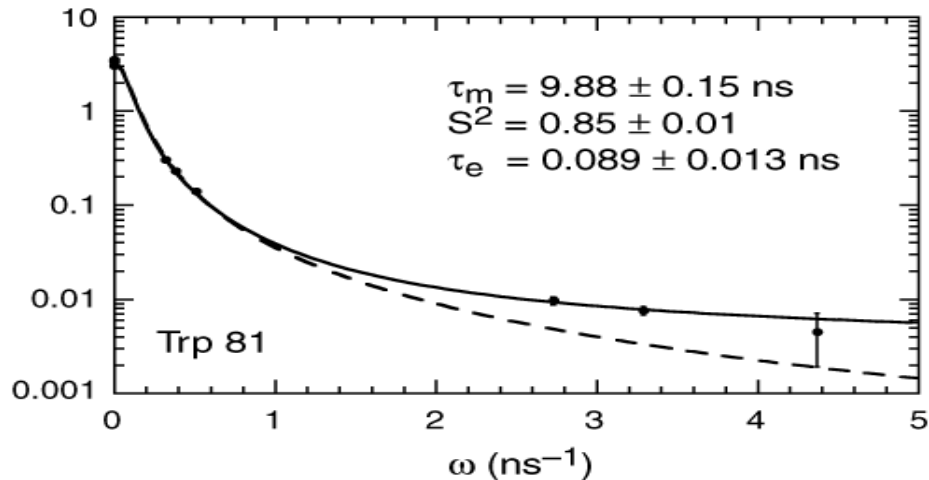
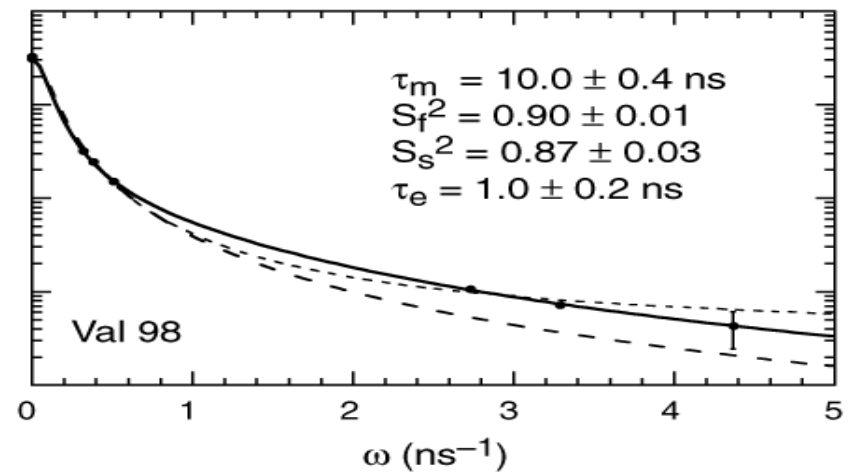
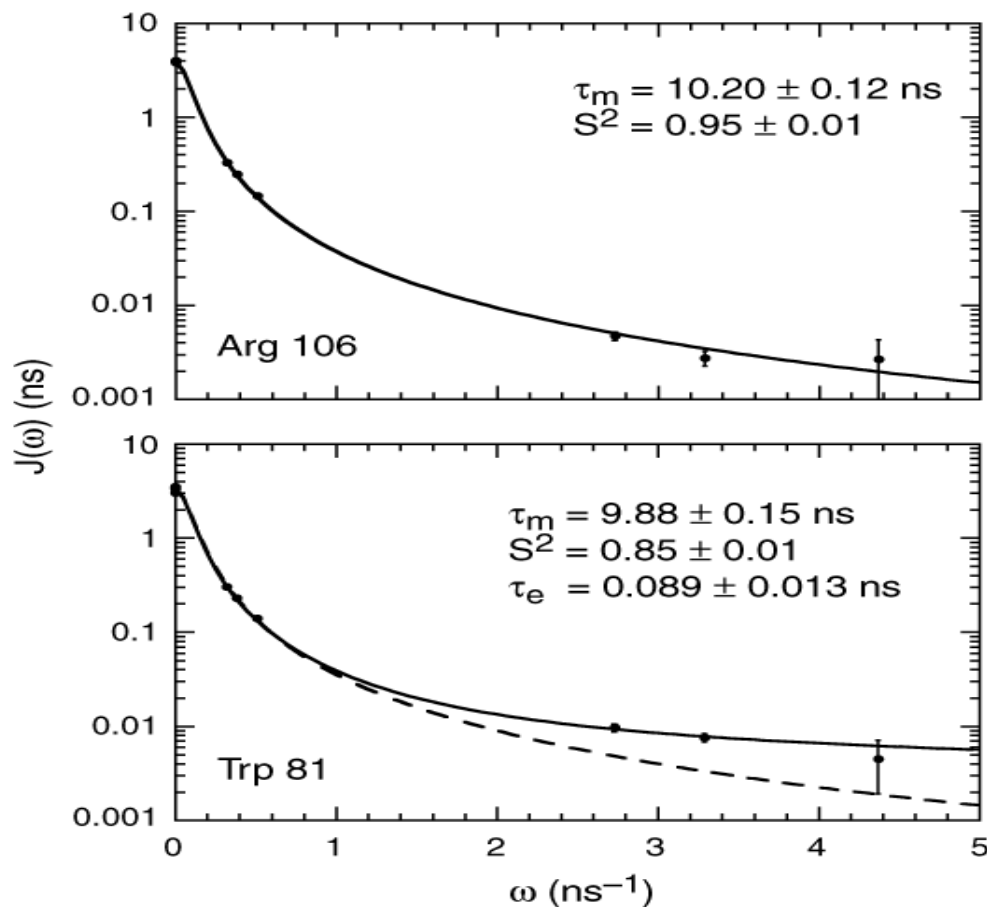
S^2 is the square of the generalized order parameter

τ_e is the correlation time for internal motions

Model Free Dynamic Parameters from Laboratory Frame (R_1 , R_2 , NOE) Relaxation

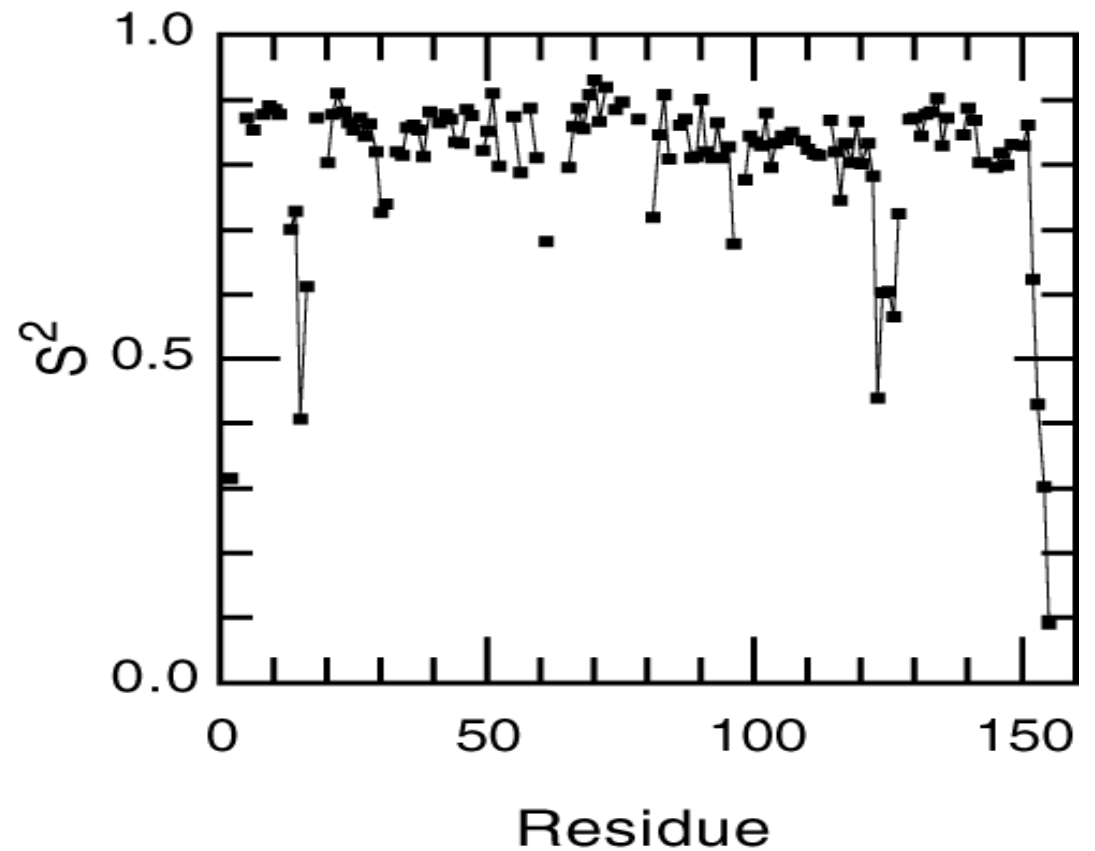
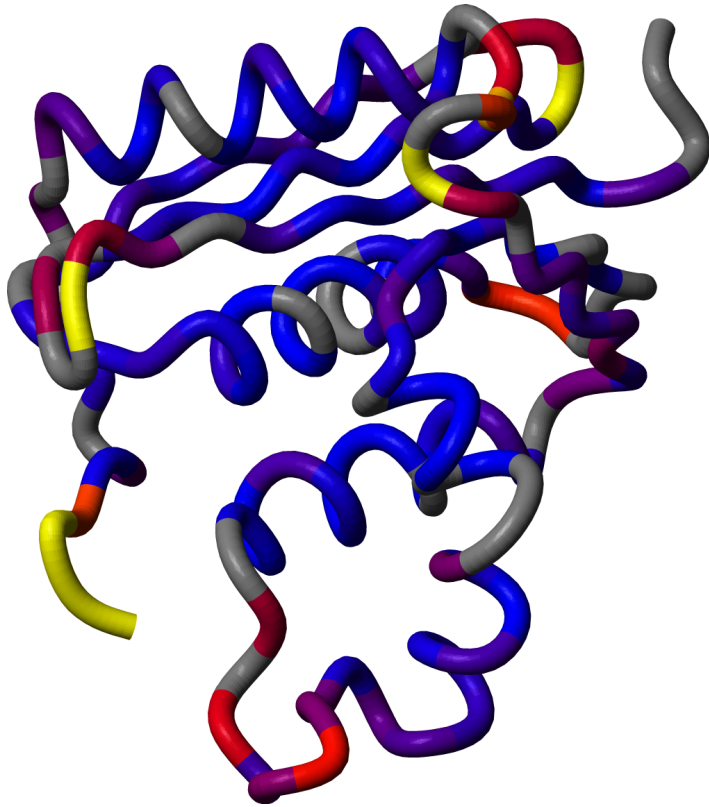


E. coli RNase H Spectral Density Functions

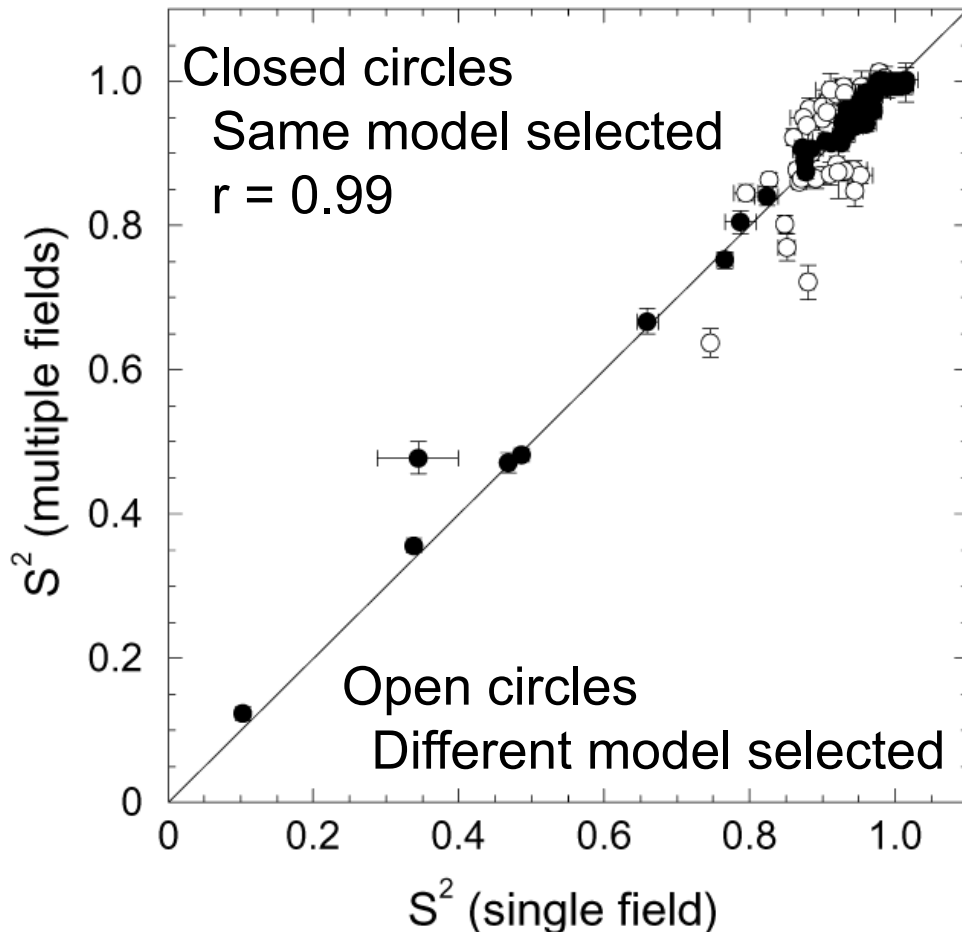


$J(\omega)$ obtained from reduced spectral density mapping using ^{15}N relaxation data at three static magnetic fields (11.7, 14.1 and 18.8 T).

Backbone ^{15}N order parameters



Reproducibility of S^2 for *E. coli* RNase H



Model-selection

F-test: A. M. Mandel, M. Akke, A. G. Palmer, *J. Mol. Biol.* **246**, 144-163 (1995).

AIC: E. J. d' Auvergne, P. R. Gooley, *J. Biomol. NMR* **25**, 25-39 (2003).

Differences arise due to difficulties in fitting R_{ex} when only single field data are available and better fitting of internal correlation times when > 1 field data are available.

Applications

Entropy of intramolecular conformational fluctuations from change in order parameters between apo and liganded protein states:

$$\Delta S_p = -k_B \sum_n \ln \frac{3 - (1 - 8S_{2n})^{1/2}}{3 - (1 - 8S_{1n})^{1/2}}$$

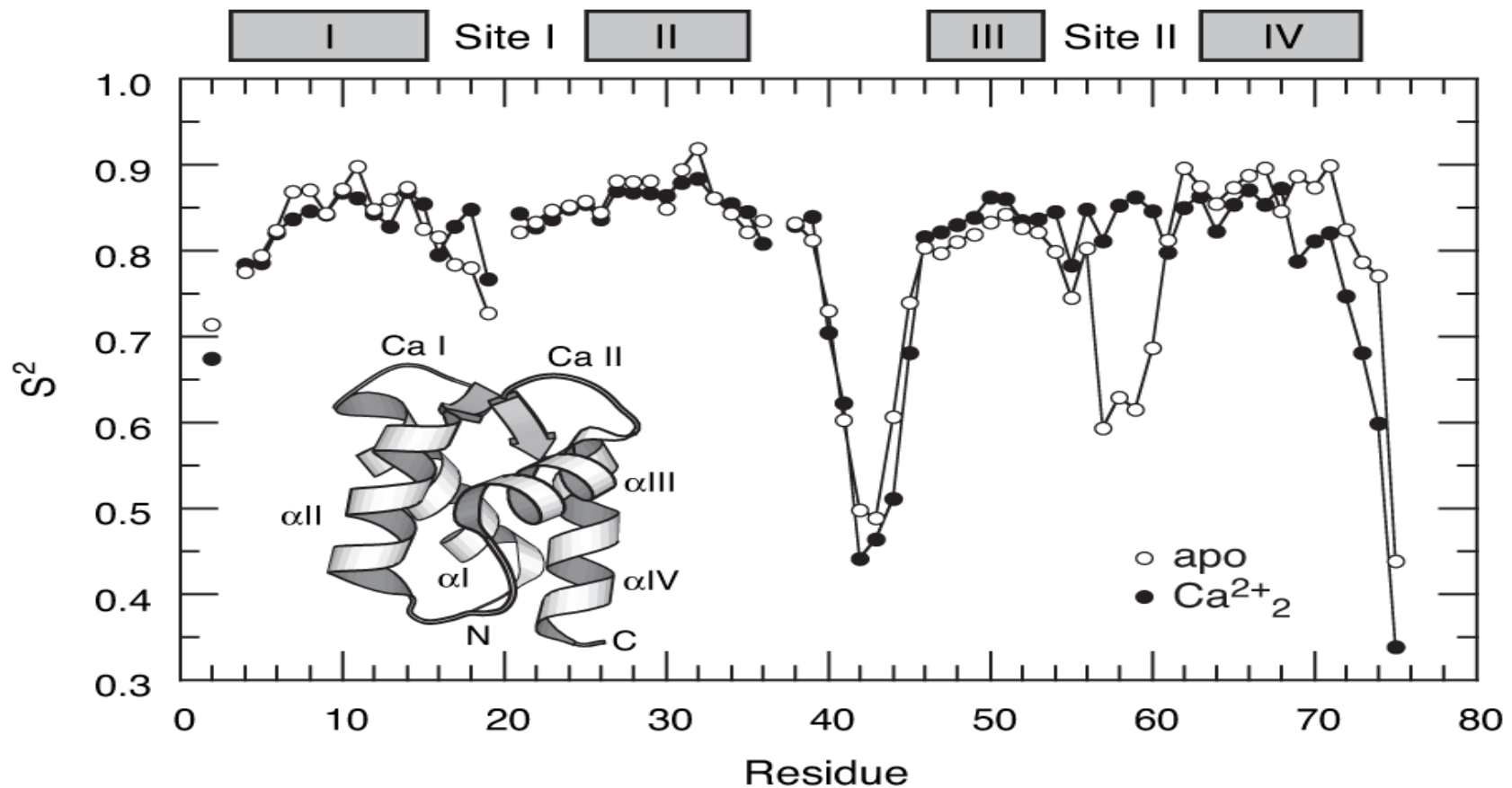
M. Akke, et al., *J. Am. Chem. Soc.* **115**, 9832-9833 (1993).

D. Yang, L. E. Kay, *J. Mol. Biol.* **263**, 369-382 (1996).

See also:

F. Massi, A. G. Palmer, *J. Am. Chem. Soc.* **125**, 11158-11159 (2003).

Backbone ^{15}N order parameters in Calbindin $\text{D}_{9\text{k}}$



Slow Dynamics and Conformational Exchange

ZZ-exchange or NOESY experiments for slow exchange with resolved resonances for each site

Lineshape analysis is most applicable near intermediate exchange when lineshape depends most strongly on exchange process

CPMG and $R_{1\rho}$ rotating frame experiments for faster processes or when only a single resonance is observable due to skewed site populations

Multiple quantum relaxation provides information on >1 spin

(Hopefully) Useful Points

Experiments conducted at different temperatures, ligand-protein ratios, etc. are very helpful in defining exchange parameters.

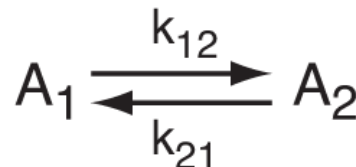
Determine R_2^0 (exchange free rate constant) from relaxation interference rate constant, B_0 dependence of $R_2 - R_1/2$, or HEROINE to simplify data analysis (initial dispersion regime).

More information is available for systems outside of the fast exchange limit.

CPMG and R_{1r} experiments are very similar theoretically and differ practically in the time scale accessible to each (fastest pulsing rate or largest B_1).

Chemical Exchange Linebroadening

$$R_2 = R_2^0 + R_{\text{ex}}$$



Fast Exchange

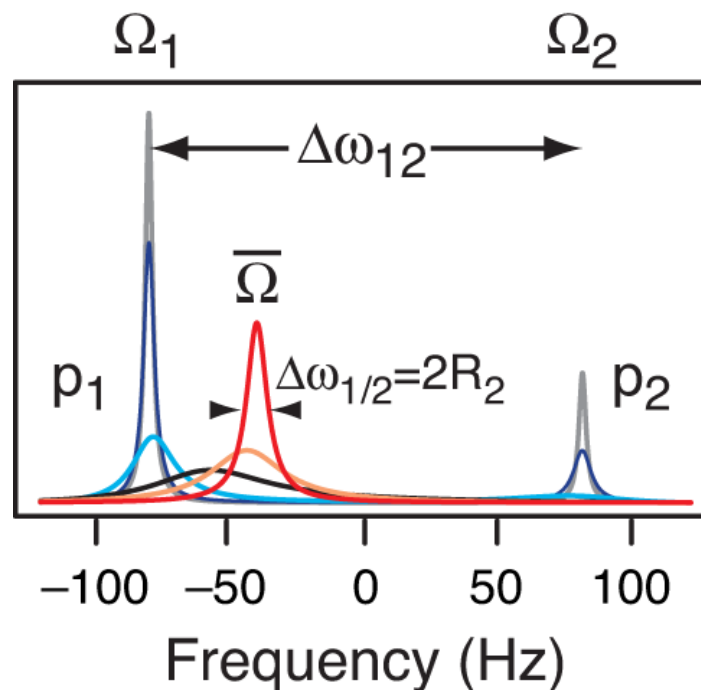
$$R_{\text{ex}} = p_1 p_2 \Delta\omega^2 / k_{\text{ex}}$$

$$\Omega = p_1 \Omega_1 + p_2 \Omega_2$$

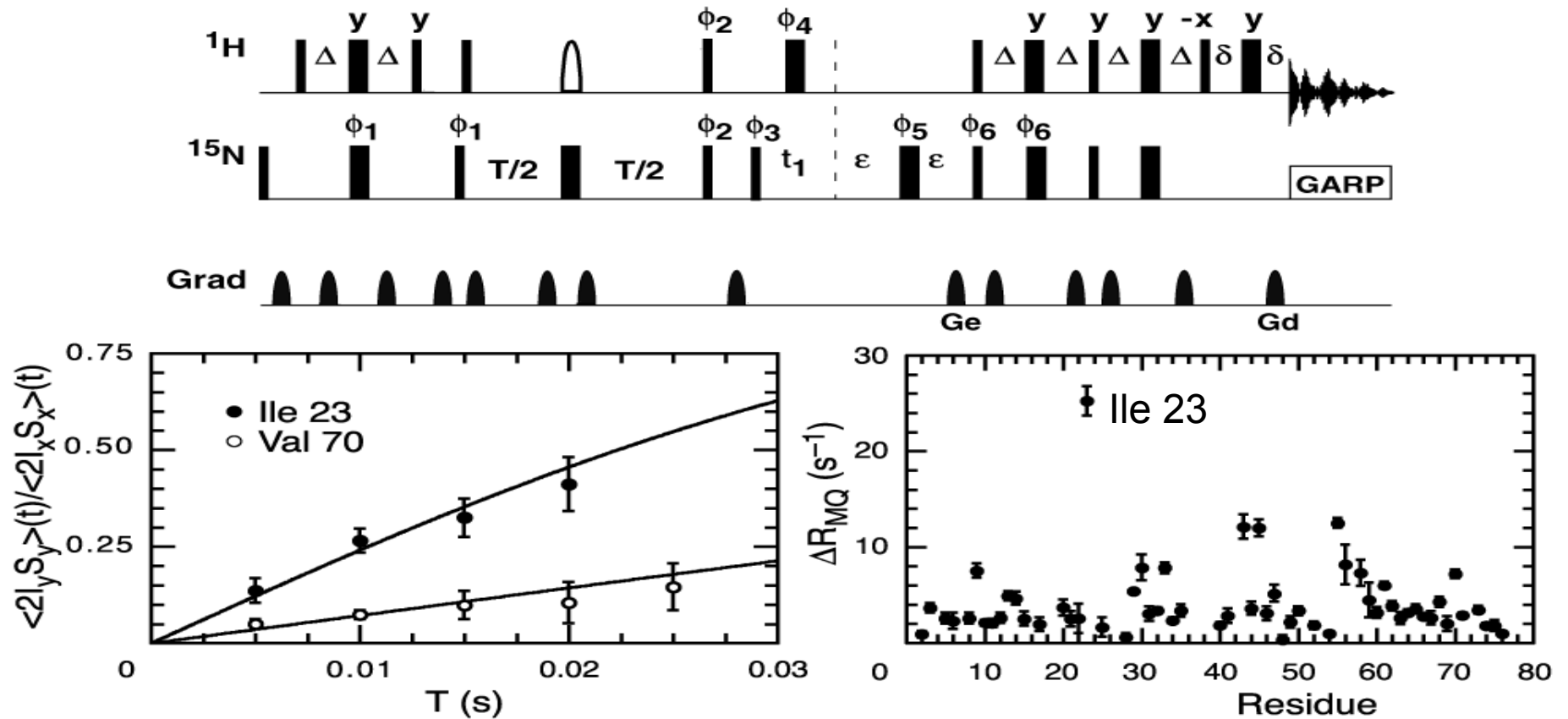
Slow Exchange

$$\begin{aligned} R_{\text{ex}}^{(\text{site } i)} &= k_{\text{ex}} (1 - p_i) \\ &= k_{12} \quad (\text{site 1}) \\ &= k_{21} \quad (\text{site 2}) \end{aligned}$$

$$k_{\text{ex}} = k_{12} + k_{21}$$

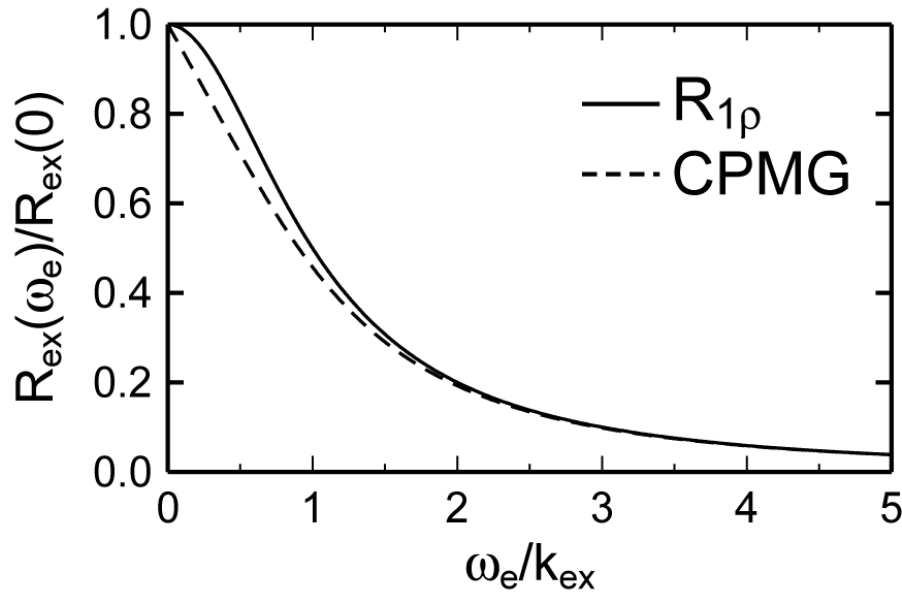


Multiple Quantum Relaxation in Ubiquitin



K. Kloiber, R. Konrat, *J Biomol NMR* **18**, 33-42 (2000).

Chemical exchange and relaxation dispersion



$R_{1\rho}$ relaxation is measured by applying an rf field with frequency ω_{rf} and amplitude ω_1 .

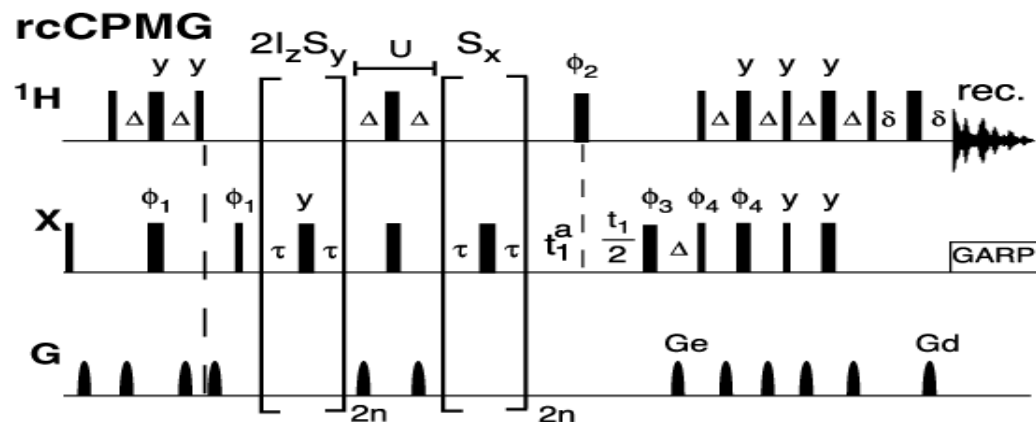
CPMG relaxation is measured by applying a train of spin echo sequences with interpulse delay τ_{cp} .

Hahn spin echo approximates $\omega_e = 0$, called $R_{ex}(0) = R_{ex}$

$$R_2(\omega_e) = R_2^0 + R_{ex}(\omega_e)$$

$$R_{ex}(\omega_e) = \frac{p_1 p_2 \Delta\omega^2 k_{ex}}{(k_{ex}^2 + (\Omega - \omega_{rf})^2 + \omega_1^2)}$$

CPMG Relaxation Dispersion

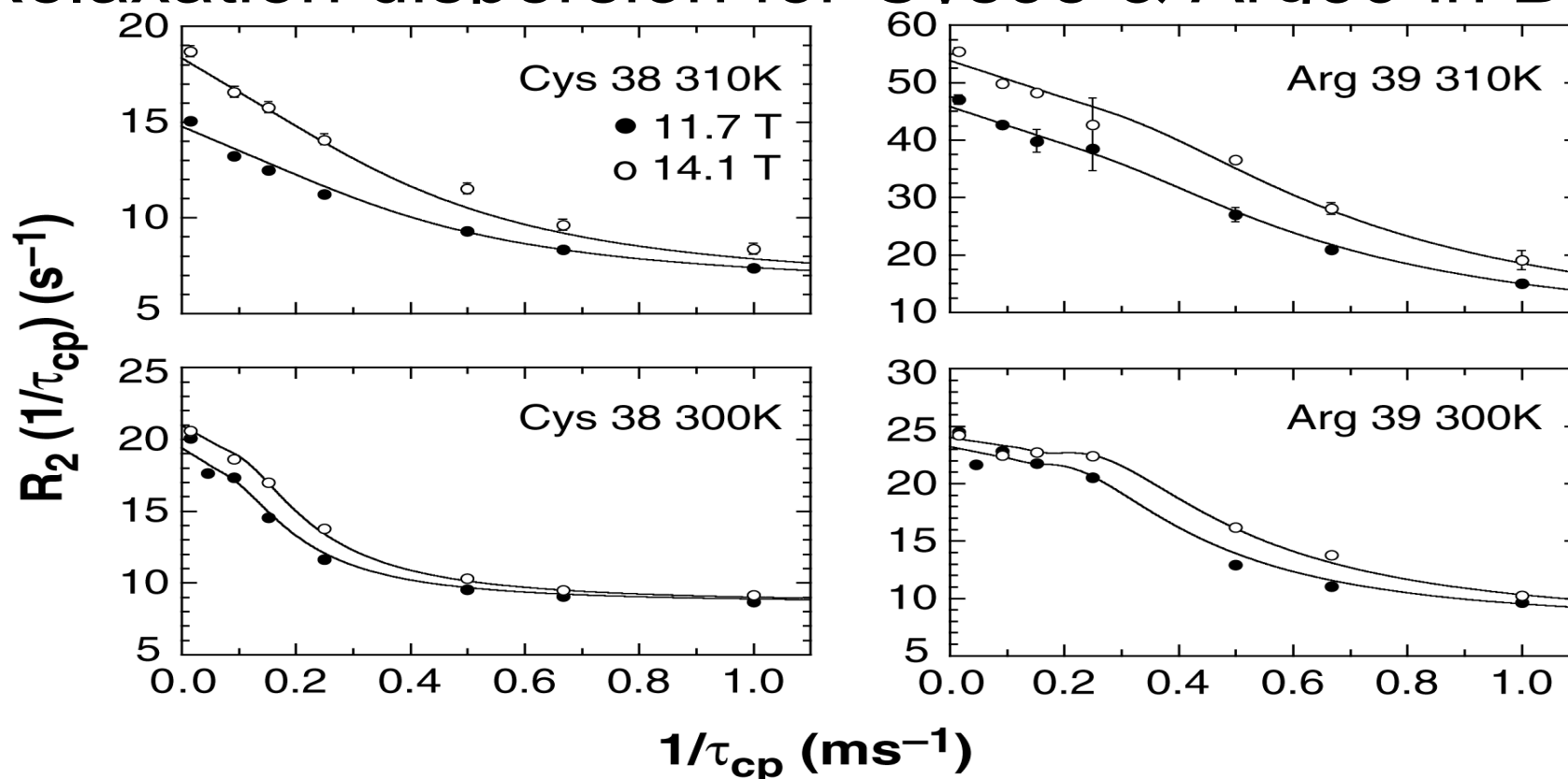


J. P. Loria, et al., *J. Am. Chem. Soc.* **121**, 2331-2332 (1999).

The sequence element U averages between in-phase and antiphase magnetization to remove the τ_{cp} -dependence of the relaxation of antiphase magnetization. The apparent value of R_2^0 is given by

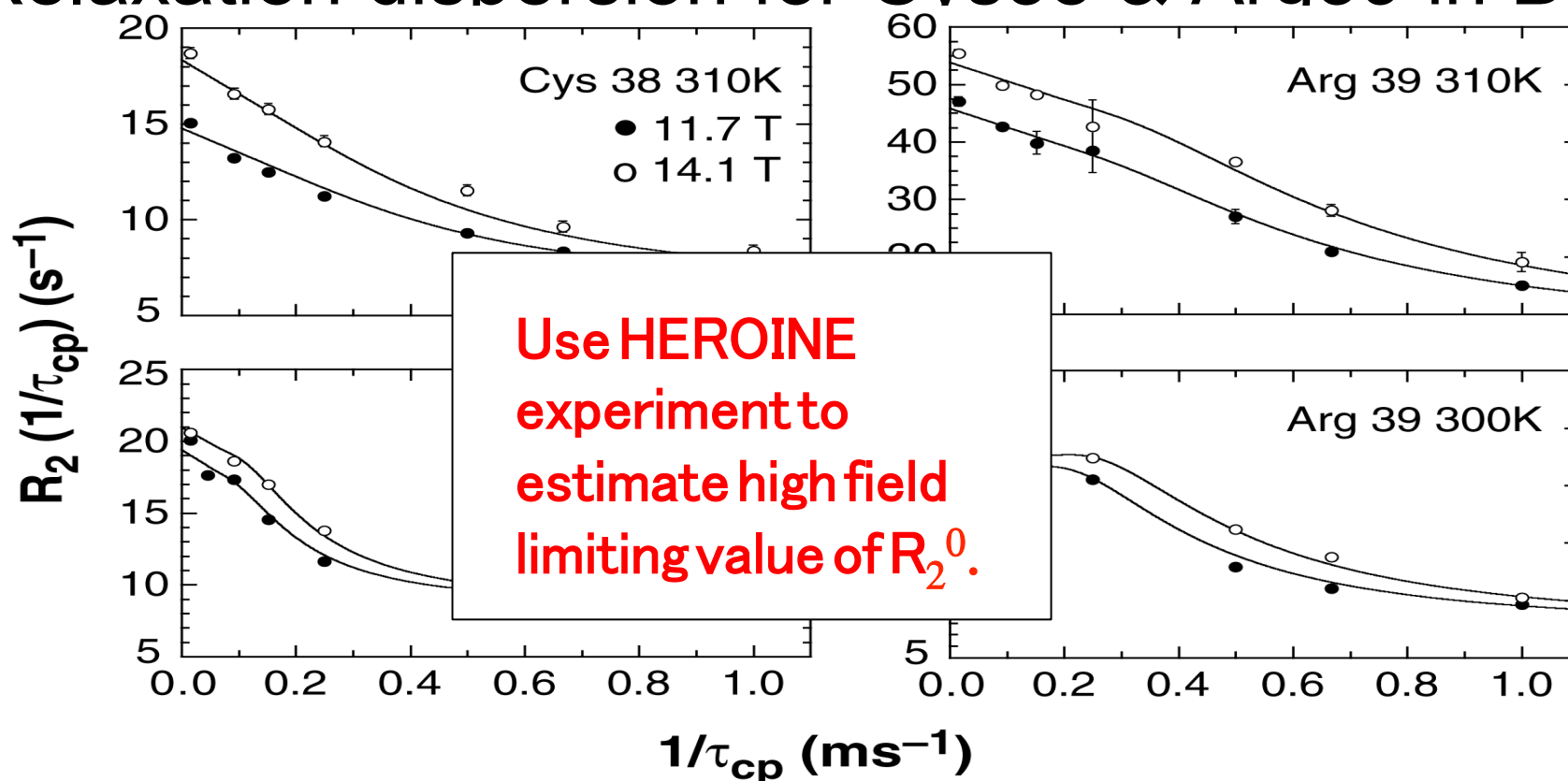
$$R_2^0 = (R_2^{\text{in-phase}} + R_2^{\text{antiphase}})/2 \approx R_2^{\text{in-phase}} + R_1^H/2$$

Relaxation dispersion for Cys38 & Arg39 in BPTI



Data at >1 magnetic field essential for fitting theoretical expressions outside the fast exchange limit

Relaxation dispersion for Cys38 & Arg39 in BPTI



Data at >1 magnetic field essential for fitting theoretical expressions outside the fast exchange limit

Structural Models for Disulfide Isomers

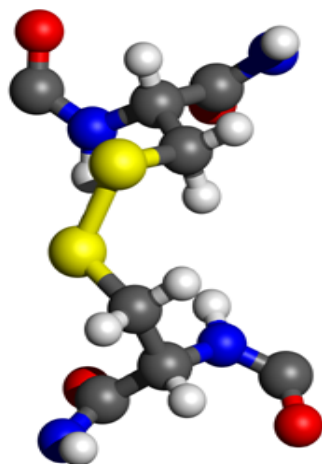
Major Species

C14 Rotamer

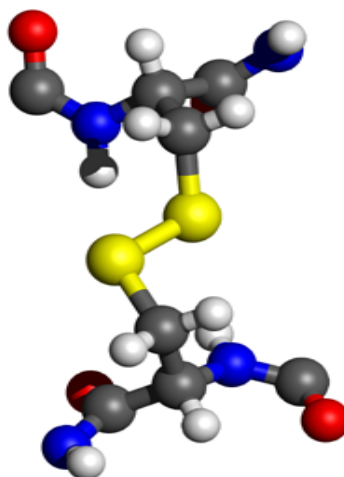
C38 Rotamer

C14 χ_1

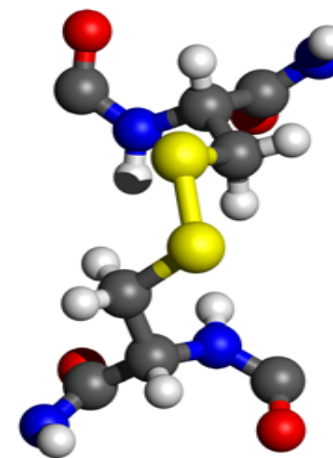
-60°



$+60^\circ$



-60°



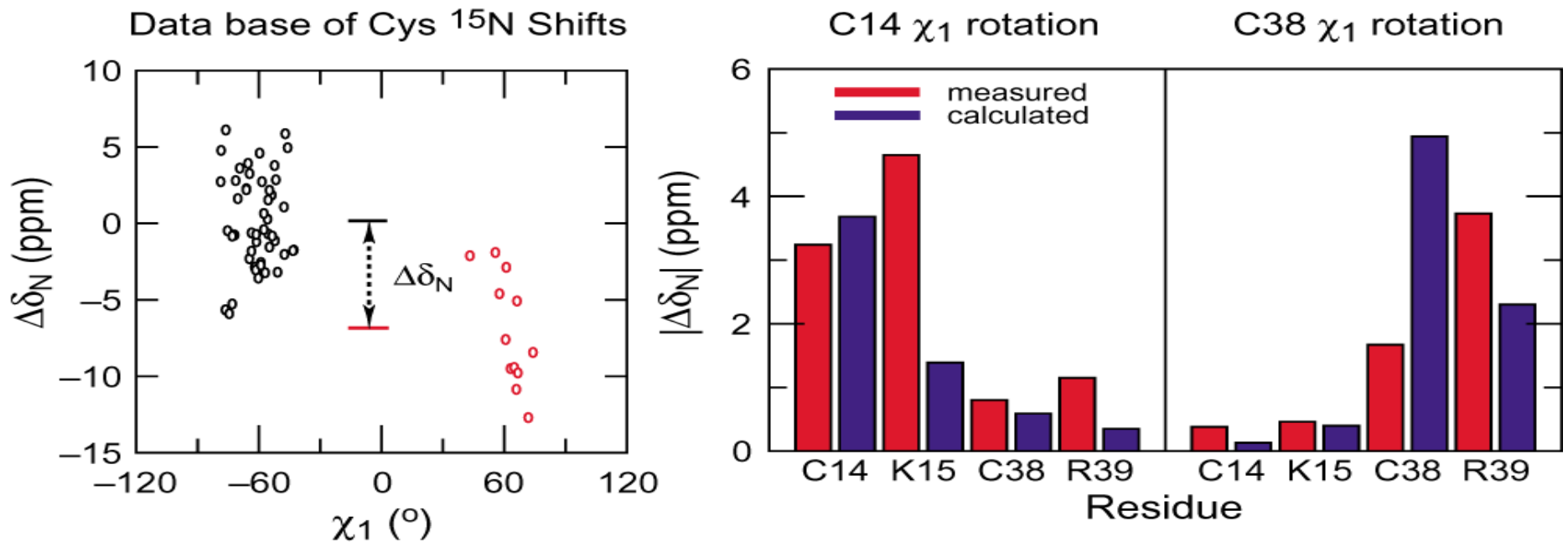
C38 χ_1

$+60^\circ$

$+60^\circ$

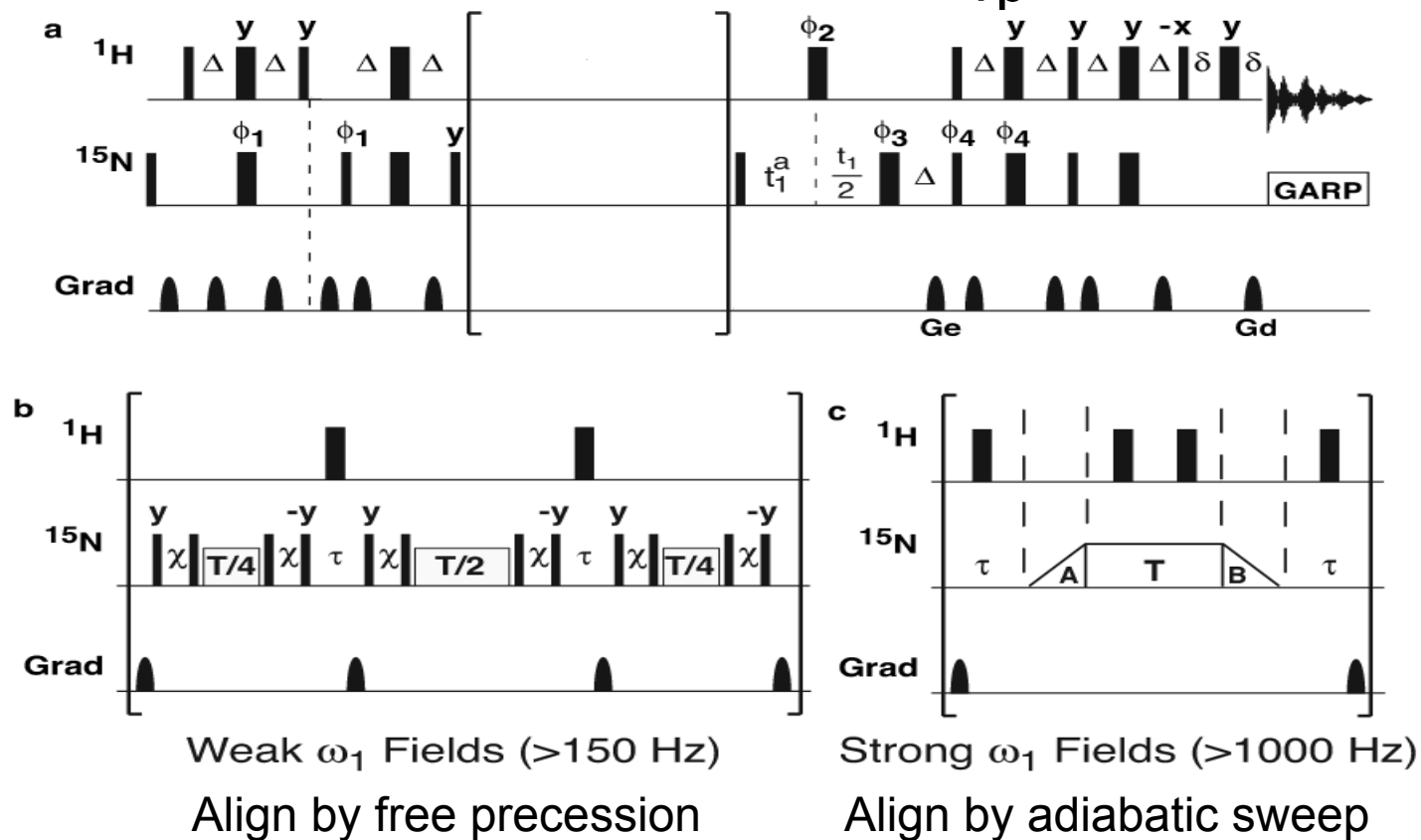
-60°

^{15}N Chemical Shifts for Cys Rotamers



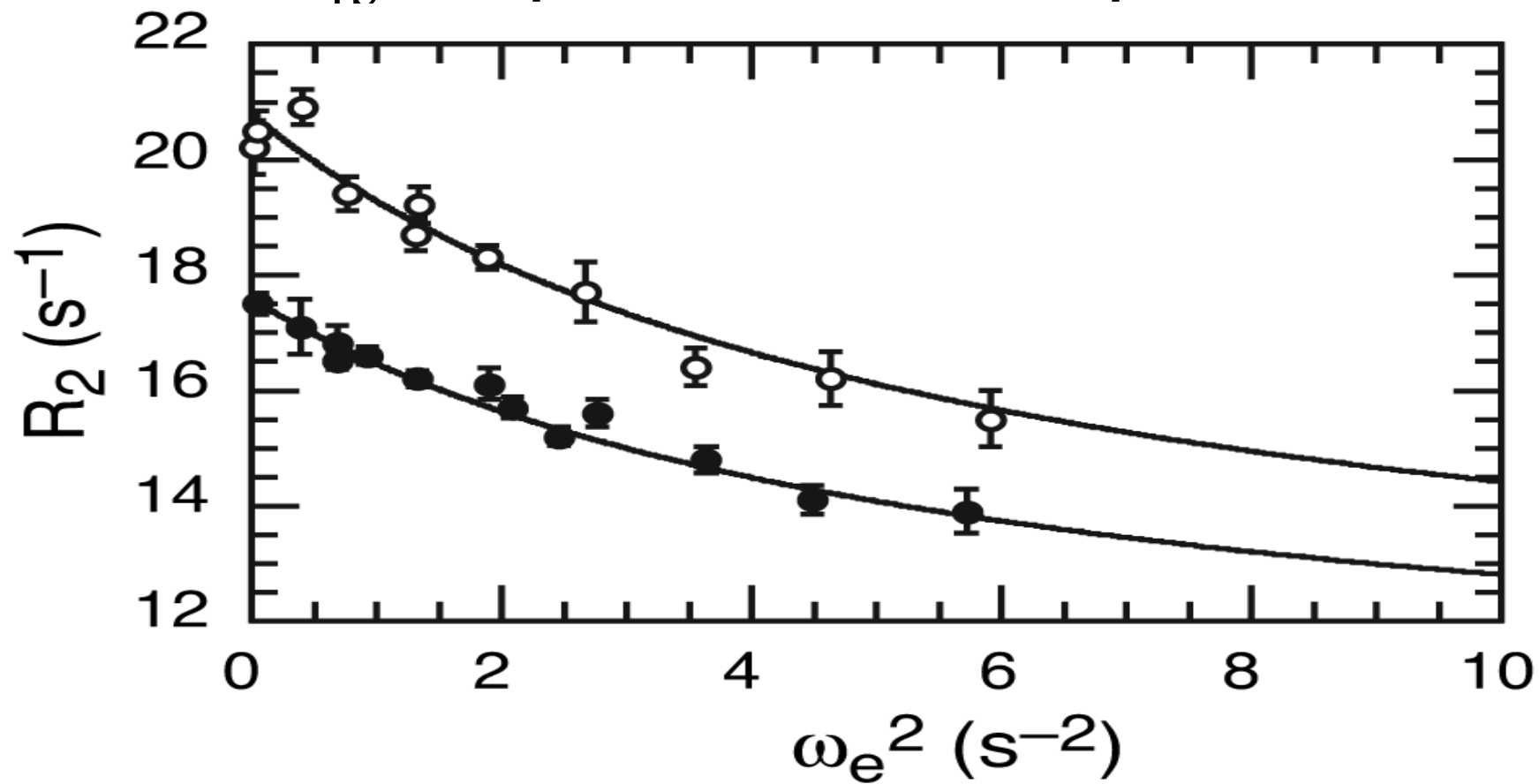
For the Cys 14 χ_1 rotation, the signs of $\Delta\omega$ for Cys14 and Lys 15 agree with the signs of the calculated shifts. The same is true for Cys 38 and Arg 39 for the Cys 38 χ_1 rotation.

Pulse Sequences for $R_{1\rho}$ Relaxation



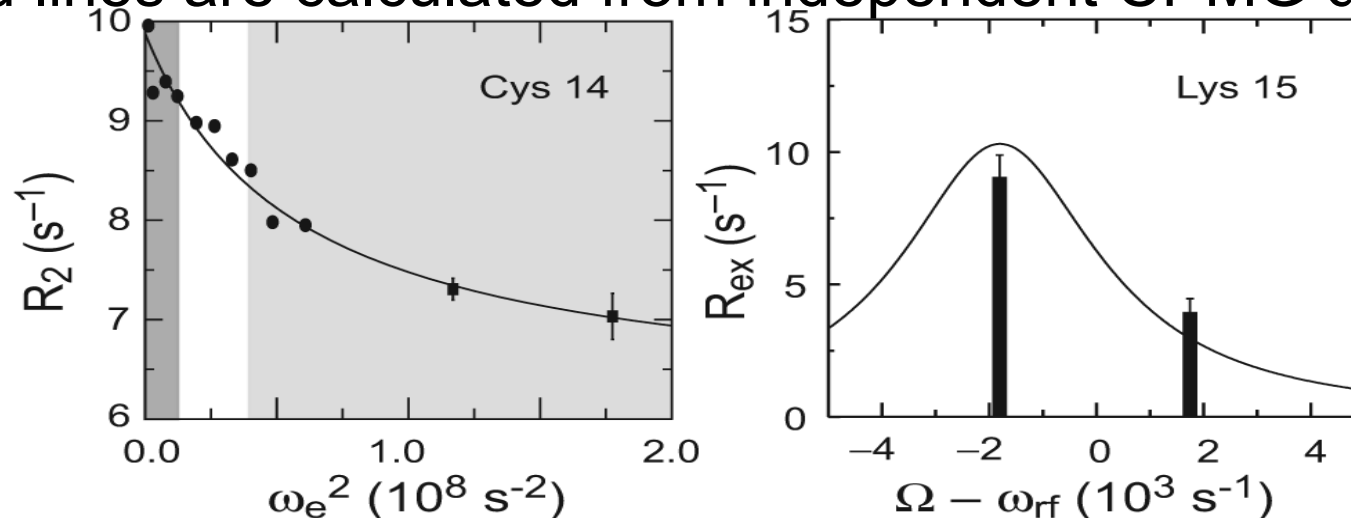
Massi, et al. (2004) *J. Am. Chem. Soc.* 126, 2247-2256

R_{10} Dispersion for Ubiquitin



Slow Exchange $R_{1\rho}$ (for BPTI)

Solid lines are calculated from independent CPMG dispersion.



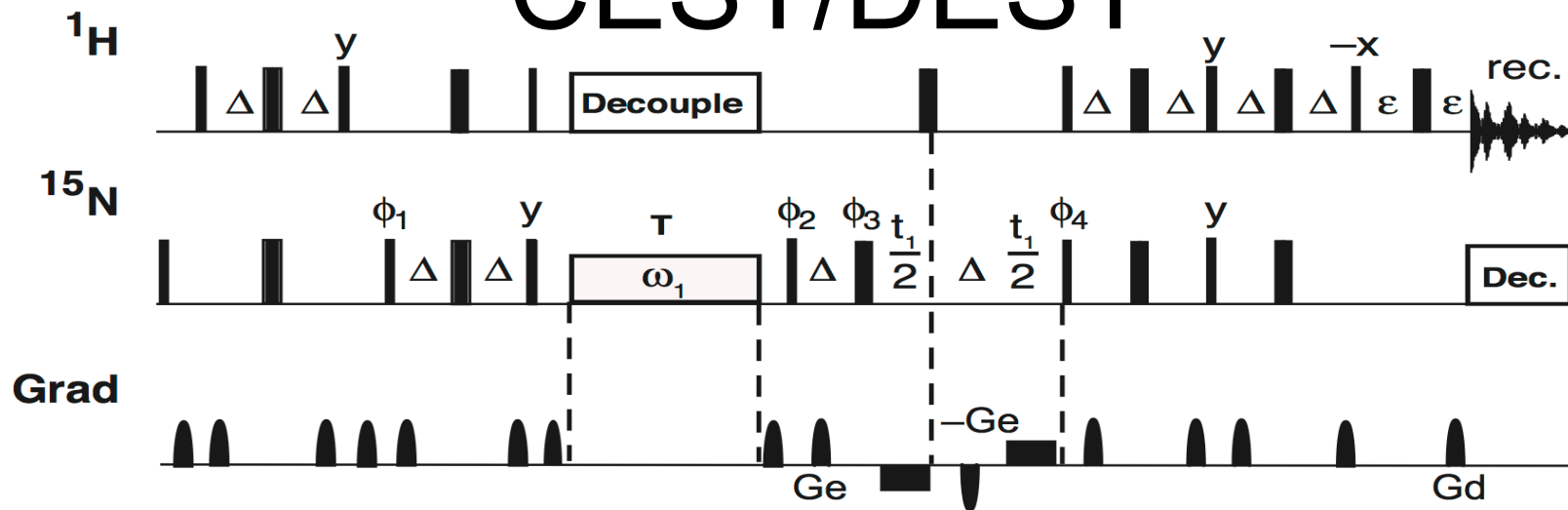
General Result for All Time Scales ($p_1 \gg p_2$)

$$R_{ex}(\omega_e) = p_1 p_2 \Delta\omega^2 k_{ex} / (k_{ex}^2 + (\Omega_2 - \omega_{rf})^2 + \omega_1^2)$$

Trott and Palmer (2004) J. Magn. Reson. 170:104-112.

Miloushev and Palmer (2005) J. Magn. Reson. 177:221-227.

CEST/DEST

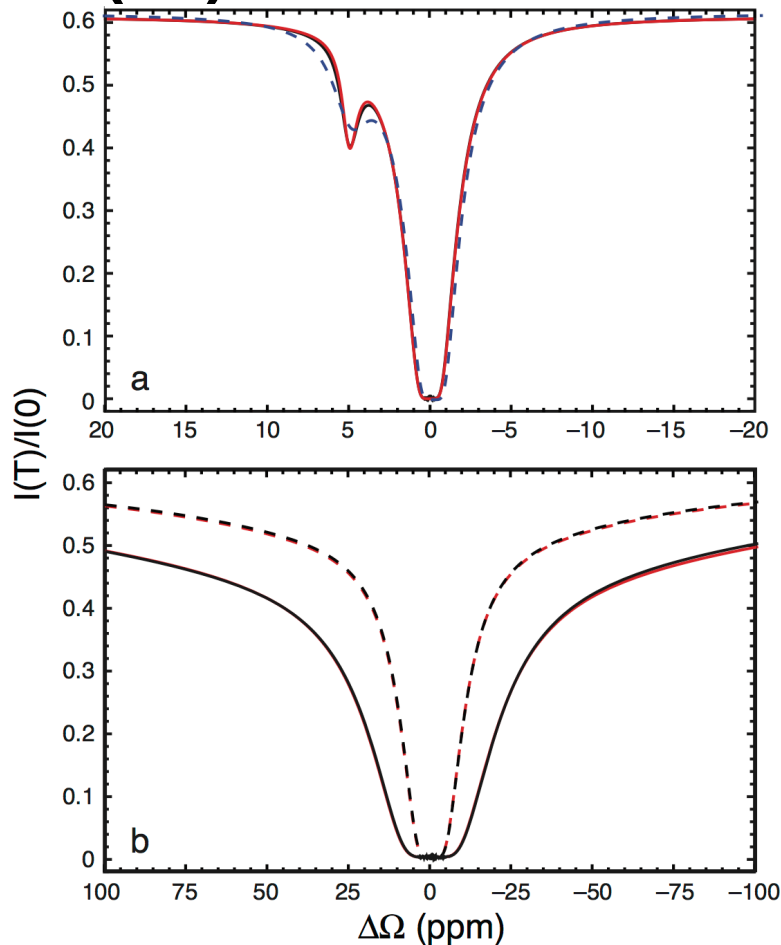


Both experiments can be regarded as $R_{1\rho}$ experiments with very weak rf fields

$$I(T)/I(0) = \cos^2\theta \exp(-R_{1\rho} T)$$

Palmer, JMR 241:3-17 (2014)

(a) CEST and (b) DEST Profiles



$$k_{ex} = 50 \text{ s}^{-1}, p_2 = 0.015$$

$$\Omega_1 = -0.076 \text{ ppm}, \Omega_2 = 5 \text{ ppm}$$

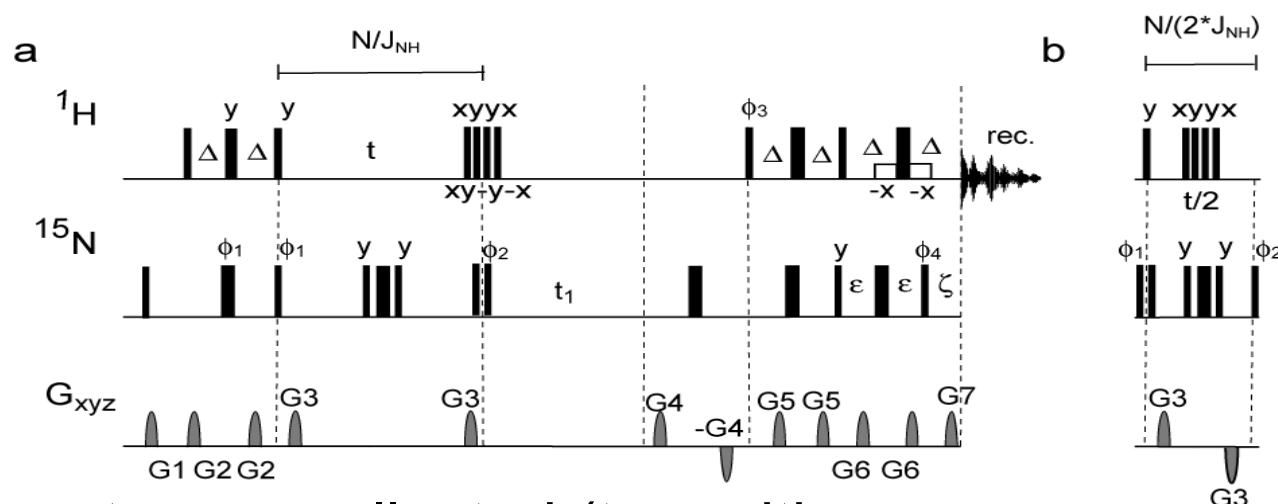
$$T = 0.48 \text{ s}$$

In (a) $R_{11} = R_{12} = 1 \text{ s}^{-1}$, $R_{21} = R_{22} = 20 \text{ s}^{-1}$, $\omega_1/2\pi = 25 \text{ Hz}$.

In (b) $R_{22} = 20,000 \text{ s}^{-1}$ and (dashed) $\omega/2\pi = 150 \text{ Hz}$ and (solid) $\omega_1/2\pi = 300 \text{ Hz}$.

(black) numerical solutions; (red) $R_{1\rho}$ approximations

TROSY-Interference Rate Measurements



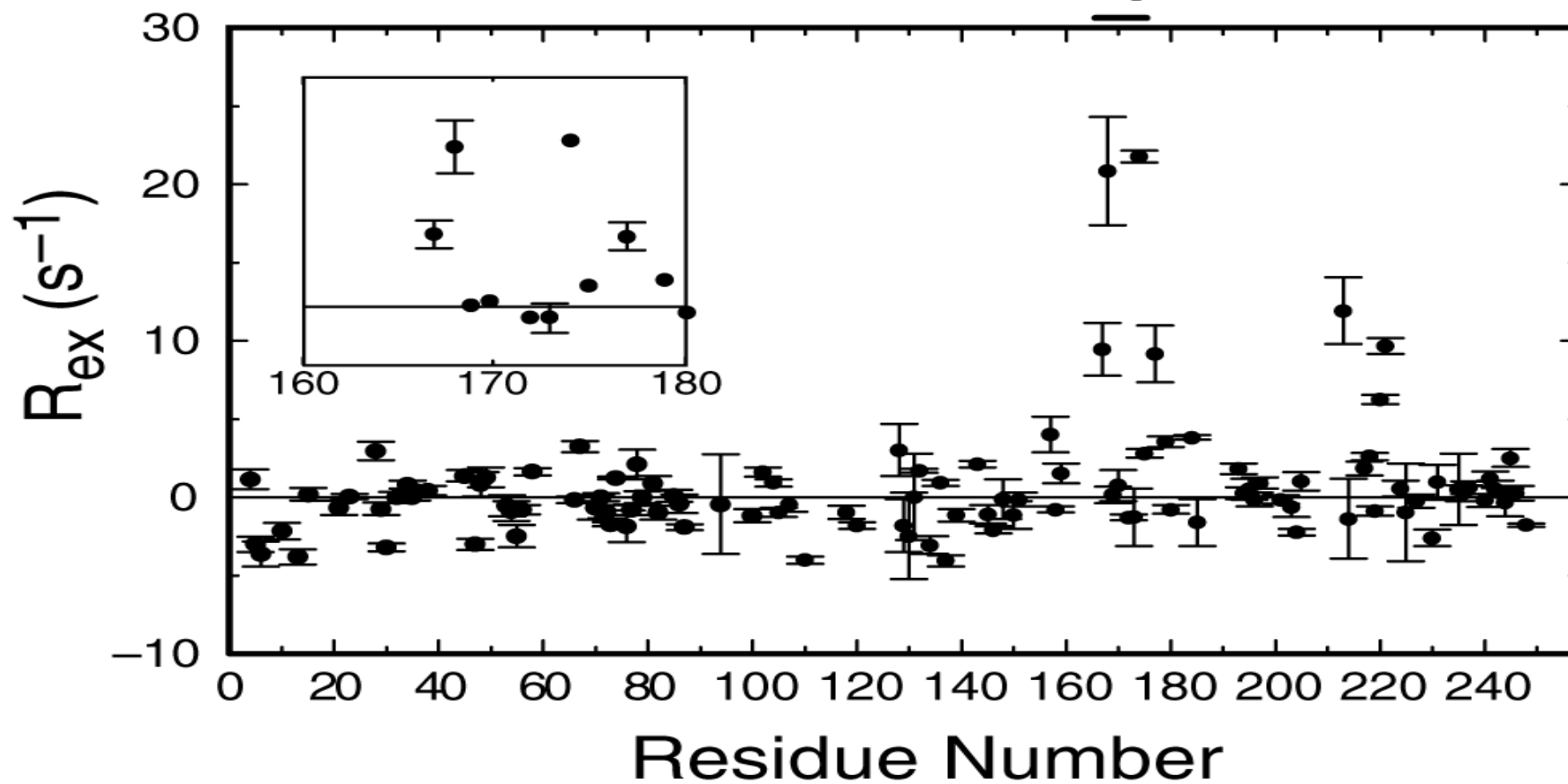
Three spectra are collected (two with sequence a and one with b). All spectra have identical intensities at $t = 0$, so relaxation rates can be obtained by appropriate ratios of intensities:

$$a(xy-y-x) = \text{TROSY } R_2 \quad a(xyyx) = \text{anti-TROSY } R_2 \quad b = 2I_z S_z$$

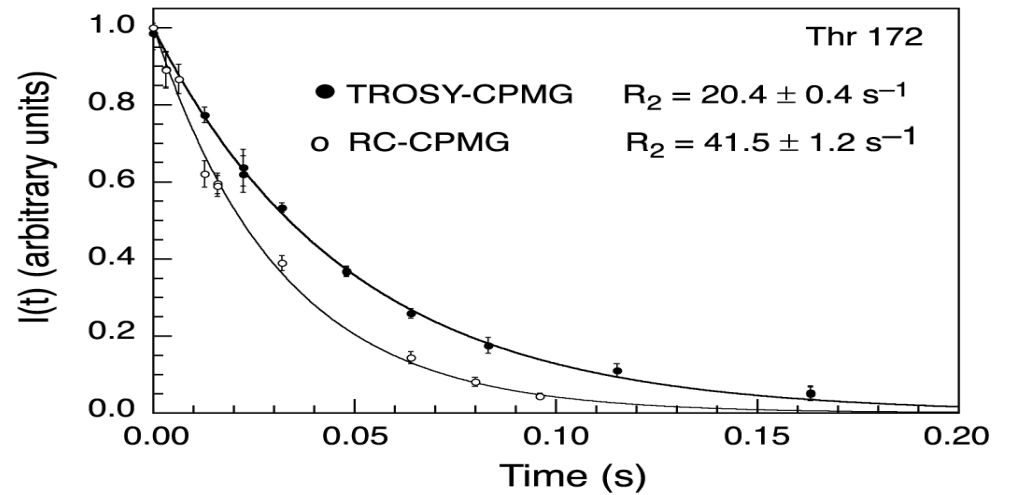
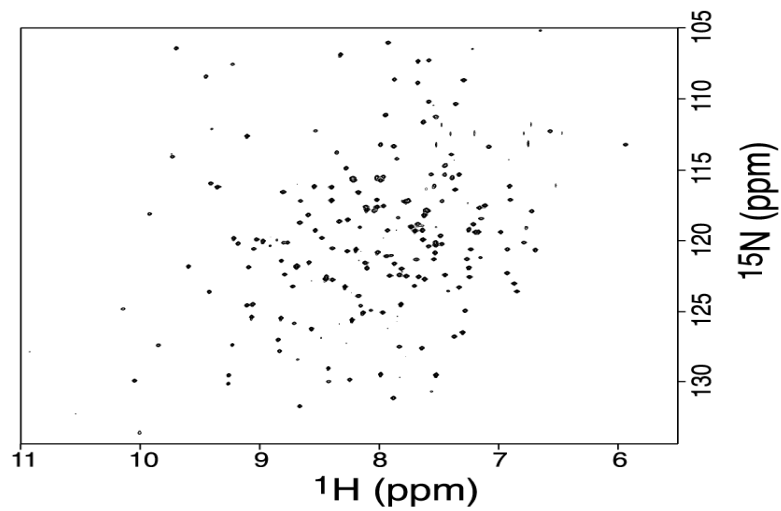
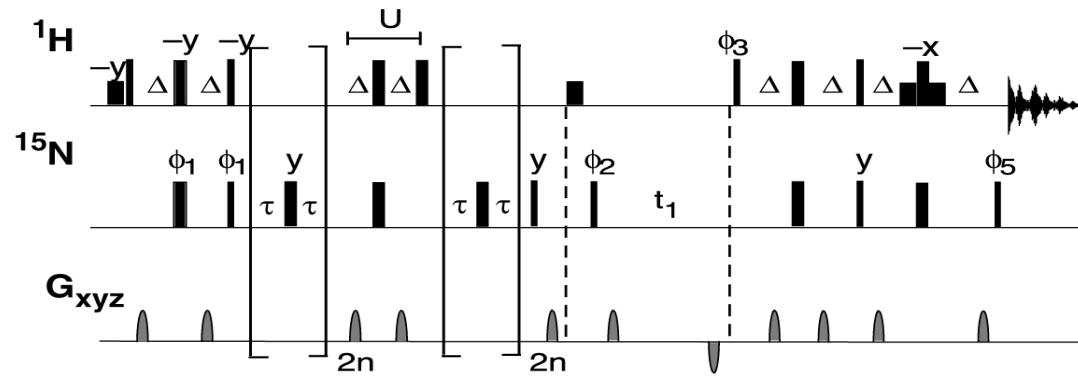
$$R_{\text{ex}} = [R_2^{\text{TR}} - R(2I_z S_z)/2] - (k - 1) h_{xy} \quad 2h_{xy} = R_2^{\text{TR}} - R_2^{\text{aTR}}$$

Chemical Exchange in G3P-ligated TIM

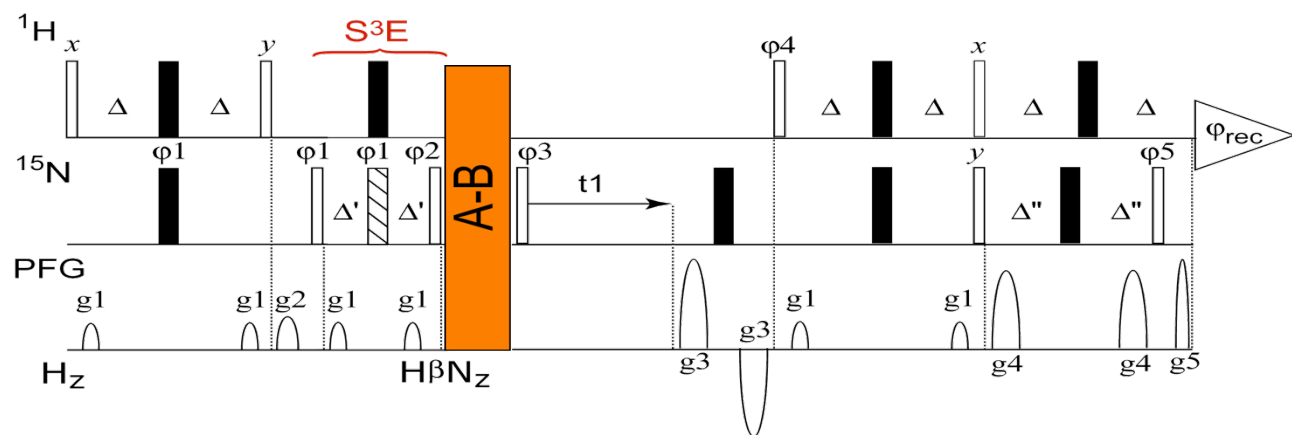
loop6



TROSY CPMG



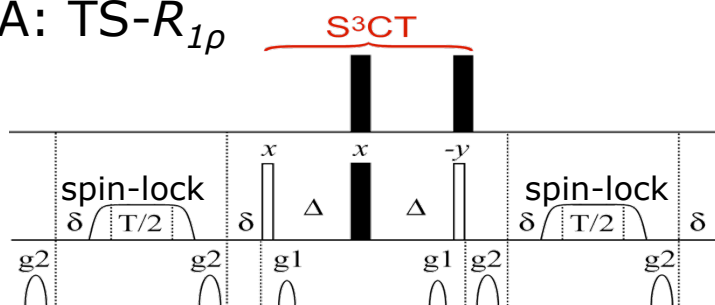
TROSY-selected off-resonance $R_{1\rho}$



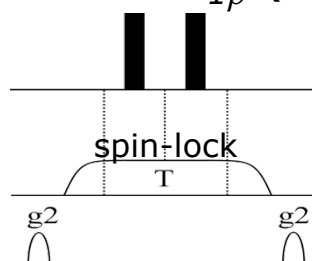
S³E: Meissner et al,
JMR 1997, 128,
92-97.

S³CT: Sorensen et
al, J. Biomol. NMR
1997, 10, 181-186.

A: TS- $R_{1\rho}$



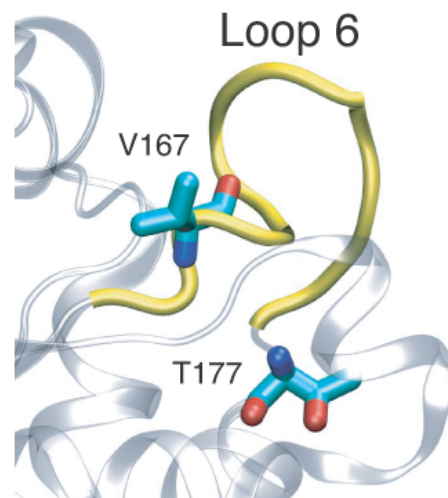
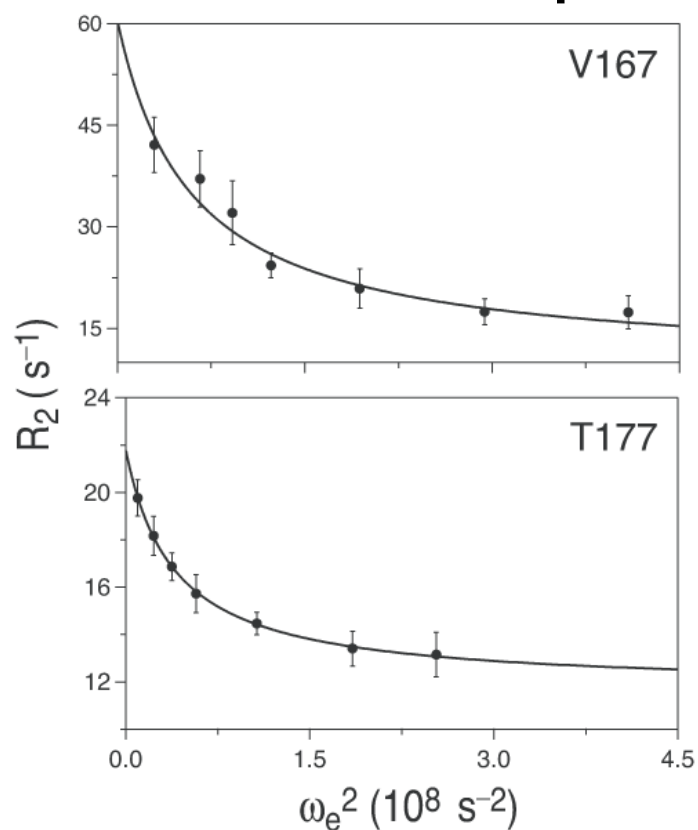
B: TD- $R_{1\rho}$ (control)



Kempf et al, JACS,
2003, 125,
12064-12065.

Igumenova and Palmer, *J. Am. Chem. Soc.* 128, 8110-8111 (2006).

$R_{1\rho}$ Relaxation Dispersion for TIM at 600 MHz



Four residues in chicken apo-TIM, V167, K174, T177, and Q179 are exchange-broadened with $k_{ex} \sim 6600 s^{-1}$.

Berlow, et al., Value of a hydrogen bond in triosephosphate isomerase loop motion *Biochemistry* (2007) 46:6001.

Conclusions

- Current NMR relaxation methods allow detailed characterization of dynamics on multiple time scales with atomic resolution using ^2H , ^{13}C , and ^{15}N spin probes.
- Applications include protein folding, ligand binding or release, multiple state equilibria, and conformational contributions to thermodynamics.
- Parameters obtained from these studies are novel constraints for models of physical or biological processes and will benefit from improved computational approaches.
- In at least some cases, >2 site chemical exchange can be characterized experimentally.
- Using TROSY-based approaches, molecules with total mass > 50 kDa are accessible.